THESIS FOR THE DEGREE OF DOCTOR OF PHILOSOPHY

Processing and properties of thermoplastic composites containing cellulose nanocrystals or wood-based cellulose fibres

LILIAN FORSGREN

Department of Industrial and Materials Science

CHALMERS UNIVERSITY OF TECHNOLOGY

Gothenburg, Sweden 2020

Processing and properties of thermoplastic composites containing cellulose nanocrystals or wood-based cellulose fibres

LILIAN FORSGREN
ISBN 978-91-7905-396-3

Doktorsavhandlingar vid Chalmers tekniska högskola
Ny serie nr 4863
ISSN 0346-718X

Department of Industrial and Materials Science
Chalmers University of Technology
SE-412 96 Gothenburg
Sweden
Telephone + 46 (0)31-772 1000

Chalmers Reproservice
Gothenburg, Sweden 2020

The path you're on looks different when you turn around

Cynthia Lewis

Processing and properties of thermoplastic composites containing cellulose nanocrystals or wood-based cellulose fibres

Lilian Forsgren

Department of Industrial and Materials Science
Chalmers University of Technology

ABSTRACT

Cellulose nanocrystals (CNC) were surface modified with dialkylamines to increase the compatibility between the CNC and the polymeric matrix, and promising results were obtained, with a 300 % stiffness increase when the mixed dispersion was compression moulded on a laboratory scale. The manufacturing process was up-scaled using water-assisted mixing in a twin-screw extruder (TSE) followed by a second compounding step and injection moulding (IM). The composites were successfully produced using conventional melt-processing techniques but these did not show the same improvement in mechanical performance, probably due to the formation of CNC aggregates. There were indications of network formation when CNC was added, especially in the case of surface-modified CNC.

Cellulose fibres and thermomechanical pulp were used as reinforcement in similar types of polymer matrices and the mixtures were similarly processed by TSE and IM. These materials were characterized with regard to appearance and durability. The discoloration of the composites due to excessive heat during processing did not significantly affect their mechanical properties, and the addition of the cellulose-based reinforcement to the polymer did not reduce its resistance to thermo-oxidative degradation compared to that of the pure matrix. In fact, the resistance to degradation was increased when lignin was present in the reinforcing element, showing a synergistic effect together with the added anti-oxidant.

Superior properties were expected for the CNC composites compared to those of the larger cellulose fibre reinforcements, but in continuous production the stiffening effects were similar regardless of reinforcement type. These results confirm that the processing method and properties strongly affect the final properties of the composite.

Keywords: *Cellulose, Cellulose nanocrystals, Composite, Thermal stability, Tensile properties, Extrusion, Injection moulding, Wood-based fibres*

LIST OF PUBLICATIONS

This thesis is based on the work performed at the Department of Industrial and Materials Science at Chalmers University of Technology between April 2016 and December 2020 under the supervision of Professors Mikael Rigdahl and Antal Boldizar. The studies presented in the following papers are referred to in the text by Roman numerals and are appended at the end of the thesis.

List of appended papers:

I. **Surface treatment of cellulose nanocrystals (CNC): effects on dispersion rheology**
K. Sahlin, L. Forsgren, T. Moberg, D. Bernin, M. Rigdahl & G. Westman
Cellulose, Volume 25, Issue 1, Pages 331-345, 2018
Reprinted with permission from Springer

II. **Composites with surface-grafted cellulose nanocrystals (CNC)**
L. Forsgren, K. Sahlin-Sjövold, A. Venkatesh, J. Thunberg, R. Kádár, A. Boldizar, G. Westman & M. Rigdahl
Journal of Material Science, Issue 54, Pages 3009-3022, 2019
Reprinted with permission from Springer

III. **Injection molding and appearance of cellulose-reinforced composites**
L. Forsgren, J. Berglund, J. Thunberg, M. Rigdahl & A. Boldizar
Polymer Engineering and Science, Volume 60, Issue 1, Pages 5-12, 2020
Reprinted with permission from Wiley

IV. **The thermo-oxidative durability of polyethylene reinforced with wood-based fibres**
L. Forsgren, E. C. Boz Noyan, A. Vega, N. Yarahmadi & A. Boldizar
Polymer Degradation and Stability, Volume 181, 2020
Reprinted with permission from Elsevier

V. **Water-assisted extrusion and injection moulding of composites with surface-grafted cellulose nanocrystals – an upscaling study**
L. Forsgren, A. Venkatesh, F. Rigoulet, K. Sahlin-Sjövold, G. Westman, M. Rigdahl & A. Boldizar
Submitted for publication

CONTRIBUTION REPORT

Paper I Shared main author. The chemical preparations were performed by Karin Sahlin-Sjövold and Gunnar Westman with the support of the author. Rheological characterization was performed by the author and all the results of the characterization were analysed together with Karin Sahlin-Sjövold. The first draft of the manuscript was written together with Karin Sahlin-Sjövold and the finalizing was done in close collaboration with all the co-authors.

Paper II Shared main author. The author planned the study and prepared the specimens together with Karin Sahlin-Sjövold. The chemical characterization was performed by Karin Sahlin-Sjövold, while the author together with Abhijit Venkatesh performed all the mechanical testing. The results were analysed together. The first draft of the manuscript was written by the author in collaboration with Karin Sahlin-Sjövold and Abhijit Venkatesh and it was finalized in close collaboration with all the co-authors.

Paper III Main author. The author planned and executed most of the experimental work and the analysis of the results with the assistance of Johannes Thunberg. The surface characterization was done by Johan Berglund with the assistance of the author. The first draft of manuscript was written by the author and it was finalized in close collaboration with all the co-authors.

Paper IV Shared main author. The author planned and executed the experimental work and the analysis of the results together with Ezgi Ceren Boz Noyan. Alberto Vega and Ezgi Ceren Boz Noyan performed the mechanical testing with the assistance of the author. The results were analysed by the author and Ezgi Ceren Boz Noyan as well as the first draft of the manuscript. The manuscript was finalised in close collaboration with all the co-authors.

Paper V Main author. The author planned and executed the experimental work and analysis of the results in collaboration with Abhijit Venkatesh and with the assistance of Florian Rigolet and Karin Sahlin-Sjövold. The first draft of the manuscript was written by the author and Abhijit Venkatesh, and the manuscript was finalised in close collaboration with all the co-authors.

ABBREVIATIONS

AA – Acrylic acid

AO – Antioxidant

CF – Cellulose fibres from tissue

CNC – Cellulose nanocrystals

CT – Cellulose fibres from tissue

DMA – Dynamic mechanical analysis

DSC – Differential scanning calorimetry

EAA – Ethylene acrylic acid copolymer

FTIR – Fourier transform infrared spectroscopy

IM – Injection moulding

LDPE – Low density polyethylene

MCC – Microcrystalline cellulose

OIT – Oxidation induction time

SSE – Single screw extruder

TGA – Thermal gravimetric analysis

TMP – Thermomechanical pulp

TSE – Twin screw extruder

DESCRIPTION OF MATERIALS

Cellulose nanocrystal reinforced composites	
Aqueous dispersion with cellulose nanocrystals (at various wt. %) produced from microcrystalline cellulose, surface modified with three different groups using methoxyazetidinium salts: AzOMe-Morpholine, AzOMe-diHexyl and AzOMe-diAllyl (Paper I)	CNC MorphCNC diAllylCNC diHexylCNC
Dispersion of ethylene acrylic acid copolymer with 15 % acrylic acid content, mixed with 0.1, 1 and 10 wt. % cellulose nanocrystals, produced from microcrystalline cellulose, surface modified with three different groups using hydroxyazetidinium salts: AzOH-Morpholine, AzOH-diHexyl and AzOH-diAllyl. Dispersion mixed, air dried and compression moulded (Paper II)	EAA15 EAA15-0.1 % CNC EAA15-0.1 % MorphCNC EAA15-0.1 % diAllylCNC EAA15-0.1 % diHexylCNC EAA15-1 % CNC EAA15-1 % MorphCNC EAA15-1 % diAllylCNC EAA15-1 % diHexylCNC EAA15-10 % CNC EAA15-10 % MorphCNC EAA15-10 % diAllylCNC EAA15-10 % diHexylCNC
Dispersion of ethylene acrylic acid copolymer with 7 % or 15 % acrylic acid content, mixed with 10 wt. % cellulose nanocrystals from CelluForce, surface modified with diAllyl using hydroxyazetidinium (AzOH-diAllyl) or a carbonate reagent. Processed as in Paper II (reference)	EAA15-10 % CNC EAA15-10 % diAllylCNC EAA7-10 % CNC EAA7-10 % diAllylCNC
	EAA15-10 % diAllylCNC (Carbonate reagent)
Pellets of ethylene acrylic acid copolymer with 7 % acrylic acid content, reinforced with 10 wt.% cellulose nanocrystals from CelluForce, surface modified with diAllyl using a carbonate reagent. Water-assisted mixed and compounded in Twin screw extruder before being injection moulded (Paper V)	EAA7 EAA7-10 % CNC EAA7-10 % diAllylCNC
	LDPE LDPE-10 % CNC LDPE-10 % diAllylCNC

Wood-based cellulose fibre reinforced composites	
Pellets of low density polyethylene reinforced with 5 wt.% or 20 wt.% thermomechanical pulp or cellulose fibres (tissue), with or without added Irganox 1010 antioxidant. Mixed and compounded using Twin screw extruder before being shaped into strips using single screw extrusion (Paper IV)	LDPE LDPE-5 % TMP LDPE-20 % TMP LDPE-5 % CT LDPE-20 % CT LDPE+AO LDPE+AO-5 % TMP LDPE+AO-20 % TMP LDPE+AO-5 % CT LDPE+AO-20 % CT
Pellets of ethylene acrylic acid copolymer with 7 % acrylic acid content, reinforced with 20 wt.% cellulose fibres (tissue). Mixed and compounded by Twin screw extrusion before being injection moulded at three different temperatures (Paper III)	EAA7 170 °C EAA7 200 °C EAA7 230 °C EAA7-20 % CF 170 °C EAA7-20 % CF 200 °C EAA7-20 % CF 230 °C

TABLE OF CONTENTS

1 INTRODUCTION

1.1 BACKGROUND

The urgent demand for sustainability both in industry and in society in general emphasises the need for low-cost, environmentally friendly materials with the potential for high-volume production. The use of fossil-based materials needs to be successively reduced, replacing them with more sustainable alternatives which still fulfil the requirements. Cellulose-based materials are an interesting and promising candidate, being renewable and biodegradable, with large availability and good mechanical properties. Cellulose-based materials have been used throughout history as construction material, fabrics, paper and packaging. Cellulose is a natural polymeric material. Other examples of natural polymers are starch, wool, proteins and DNA. Synthetic polymers started to be developed in the early 1950s. Since then, the production of synthetic polymers has increased steadily, and synthetic polymers, often called plastics, are highly incorporated into most people's everyday life. The properties and applications are vast, and the use of plastics has strongly contributed to the development of today's society and technologies, for example, in revolutionizing the packaging industry, increasing the shelf-life of groceries and hence decreasing food waste, and in reducing weight of load-bearing constructions in the automotive and aero industries to reduce fuel consumption. Despite the positive contributions of plastics in society, there are nevertheless drawbacks regarding: the fossil origin of most plastics in use today and the sometimes harmful substances used as additives in polymers, but the greatest concern with plastics is the pollution caused by littering, i. e. their accumulation in nature and the oceans, affecting living creatures to an extent that is not yet fully understood but definite. The collection and waste management of polymers is vital but it is also important to reduce the amount of plastics used, especially for excessive packaging or single-use products which can be replaced by more sustainable materials, which would be beneficial to reduce the environmental pollution.

Reinforcing elements can be introduced to increase the stiffness and strength of the usually ductile polymers. Commonly used reinforcing elements are glass fibres or carbon fibres, both conventionally produced from a non-renewable resource. The use of cellulose-based reinforcements in thermoplastics was proposed in the 1970s[1–5] and they have the potential to replace fossil-based materials in polymer composites in a number of applications. The automotive, construction and packaging industries have all increased the use of natural fibre composites during the last two decades[6–11], motivated by their relatively low density and interesting mechanical properties, being renewable, biodegradable and abundantly available at a relatively low cost. There are however problems in using cellulose as a reinforcing element in a polymer matrix; the mixing of a hydrophilic cellulose with a

hydrophobic polymer leads to aggregation and makes the dispersion of the fibre difficult. Fibre breakage, thermal degradation during processing and poor adhesion between the reinforcement and matrix are also difficulties that affect the final properties of the composite material[12,13]. Many of these challenges are directly related to the manufacturing and processing of composites, to the continuous feeding of the reinforcement and hence to the dispersion of the reinforcement, thermal degradation and fibre breakage. The final properties of the thermoplastic composites with cellulose-based reinforcement are thus highly dependent on the processing conditions.

1.2 CELLULOSE-BASED REINFORCEMENTS

Cellulose is the most abundant polymer on earth, with an annual production estimated to be over 10^{11} tons[14], produced by photosynthesis in plants using sunlight. Cellulose can also be found in algae, fungi and some species of bacteria, but most of the cellulosic material is found in the plant cell wall. The properties of the cellulose fibre vary among different sources, and depend on the size, shape, crystallite content, orientation and thickness of the cell walls[15]. Cellulose compounds from wood are of special interest since the forest industry is large in Sweden, with 2/3 of the country covered by forest[16]. Approximately 40 % of the wood structure is cellulose, and the other main components are hemicelluloses (about 30 %), lignin (about 30 %) and some minor amounts of extractives. These components can be separated in various ways, following currently used processes within the pulp and paper industry[17,18].

The cellulose molecule consists of a long linear homo-polysaccharide chain, which can be up to 20000 monomer units long depending on the source[19,20]. The chains have both crystalline and amorphous regions forming cellulose nanofibrils, which are aligned and aggregated together into microfibrils. The hydroxyl groups (-OH) of cellulose form hydrogen bonds both within the molecule and between the molecules, thus forming strong crystalline regions. Cellulose plays a critical role in maintaining the structure of the plant cell wall by contributing both strength and stiffness, making it possible for tall thin structures and stems to withstand the stresses from the environment. Although it is a polymer, it is not possible to process cellulose using thermoplastic techniques since the cellulose decomposes at temperatures lower than melting.

Cellulose has been and is continuously being used in numerous applications and particularly as a construction material throughout human history. There is an ongoing development of the use of this multifaceted material in new applications involving different processing techniques and treatments and also as an additive in other types of materials, cellulose can for example be incorporated into concrete and insulating materials, it can be used as a thickener in food and viscous products like paint and it can serve as a reinforcement or filler in thermoplastics, elastomers and thermosets[21–23]. The concept of using cellulose-based or

wood-based fillers in polymer composites is not new, and a substantial amount of work has aimed at optimizing the use of natural fibres in many applications[24]. Cellulose or natural fibres have been of interest as reinforcement in composites for several years and they are already applied in automotive and aircraft components, packaging, electrical components, sporting equipment and the biomedical industry[10].

Combining cellulose with a polymer gives great opportunities to improve the mechanical properties of inherently rather weak and flexible polymers and at the same time reduce the need to use fossil-based materials. It may also be possible in the future to replace some glass-fibre reinforcements with cellulosic materials. Cellulose has potentially good mechanical properties as a reinforcing element with high specific stiffness and high strength. In addition to its promising mechanical property profile and its low density, the main advantages of cellulose are its renewability, biodegradability, low abrasion towards processing equipment and its almost unlimited availability to a low cost if replanting is continuously maintained.

However, when cellulose is used as a reinforcing material in a polymer matrix, some challenges must be faced. The hydrophilic nature of cellulose makes it prone not only to absorb water but also to repel the most conventionally used polymers due to their, often, hydrophobic nature. The ability to absorb moisture impedes processing since high moisture levels are not desired, and this may also contribute to the formation of aggregates. Fibre aggregates are hard to break up and this makes it difficult to distribute the fibres uniformly in the polymer matrix. The mismatch in hydrophilic/hydrophobic character between cellulose and most plastics can also result in a weak interphase between the two components and thus to adhesion problems and a reduced reinforcing effect[12,13]. Another problem when cellulose is used as a reinforcement in a polymer matrix is the thermal stability of the cellulose. Elevated temperatures are needed when processing thermoplastic materials, but degradation of the cellulose may start below the required processing temperature, depending on the choice of polymer matrix. Thermal degradation is also dependent on the type of fibre, the concentration, the presence of oxygen and moisture and the exposure time[25–27]. Degradation of the fibres will reduce the mechanical performance of the composite, and the surface characteristics and visual appearance of the component may change.

Cellulose or wood fibres can be used in different grades as a reinforcing element, giving different properties and at different costs. There are in principal two ways to separate fibres from the wood matrix, by either a chemical or a mechanical pulping process. In the mechanical pulping process, debarked wood logs or wood chips are mechanically ground resulting in a pulp with a high yield where most of the constituents of the wood are still present; cellulose, lignin, hemicellulose and some minor amounts of extractives. The chips can be pre-heated with steam to 120 °C prior to the grinding process resulting in thermomechanical pulp (TMP)[17]. The pre-heating softens the bounds between the fibres to

give a more gentle refining process and increase the proportion of whole fibres compared to fibre fragments[18]. The mechanical pulp consists nevertheless of a wide distribution of size fractions and the final properties of the pulp are dependent on the processing parameters used. The chemical pulping process separates the cellulose fibres by dissolving most of the lignin, which acts as an adhesive between the fibres. The most dominant process used for the production of chemical pulp is Kraft cooking, using sodium hydroxide and sodium sulphide. Both mechanical and chemical pulp can be further processed by bleaching.

The cellulose fibres are, as mentioned before, built up of long cellulose molecular chains divided into amorphous and crystalline regions on a nanoscale. There are in general two different types of nanocellulose; cellulose nanofibrils (CNF) produced by mechanical treatment of the cellulose fibre (often combined with a chemical treatment), and the even smaller cellulose nanocrystals (CNC) produced by acid hydrolysis of the cellulose fibre[28]. In the present study, only CNC has been considered. The CNC has been extracted by removal of the amorphous regions by hydrolysis of the cellulosic fibres/fibrils using sulfuric acid, leaving only the densely packed crystalline regions[29,30], in our case typically with needle-like crystals about 6 nm thick and 200 nm long[31]. The properties of CNC are in general dependent on the cellulose source with regard to dimension, aspect ratio and crystallinity, whereas the hydrolysis conditions determine the surface chemistry, surface charge and particle aspect ratio[28]. Nanocellulosic materials possess promising mechanical properties due to their dense and strong structure with a greater strength and stiffness than the larger cellulose fibres, as well as a larger surface area for adhering to the matrix[9]. Values reported by Lee et. al.[32] indicate that the tensile strength of a CNC is in the range of 0.3-22 GPa and that the axial modulus is between 58 and 180 GPa, and this is the reason for the interest in using CNC as a reinforcing element in composite materials, cf e. g. Klemm et al.[33].

The hydroxyl groups (-OH) on the CNC surface provide high surface reactivity[11] and hydrolysis converts some of the surface hydroxyl groups on the CNC to negatively charged sulphate half-ester units, stabilising the CNC in aqueous dispersions and reducing the tendency to aggregate. However, the sulphate groups also promote thermal degradation through an acid catalysed dehydration process starting already at 150 °C, and this can be detrimental since the commonly used engineering polymers require higher processing temperatures[34,35]. This dehydration process can be inhibited by neutralisation by e. g. sodium hydroxide[35].

The properties of the CNC can be tailored by grafting functional groups onto the cellulose surface to reduce the hydrophilic nature of the cellulose and increase its compatibility with a hydrophobic matrix, increasing the adhesion and interactions both between matrix and reinforcement and between reinforcing elements[13,36]. The thermal stability can also be increased by chemical modifications grafted onto the sulphate groups on the CNC surface[10,37]. Börjesson and Westman[38] have summarized possible routes and processes which can be used to adjust the properties of CNC.

There is a growing interest in using cellulose-based materials as reinforcement in polymer composites, but the processing and manufacture of these materials in general needs to be better understood, and also the properties of the final material with regard to ageing and the visual appearance in terms of surface characteristics and discoloration or yellowing associated with the formation of chromophores due to oxidation of the material. This degradation can be initiated at rather low temperatures especially with long exposure times[39,40]. The type of cellulose affects the degradation and other substituents, e.g. lignin and hemicelluloses contribute to the discoloration. The durability of cellulose-reinforced composites is affected by thermo-oxidation[41], exposure to UV radiation, moisture an oxygen in addition to elevated temperatures. The thermo-oxidative degradation is also influenced by the porosity of the composite, the physical and chemical structure of the polymer matrix and the amount and type of antioxidant present[41]. The degradation of the polymer matrix has been reported to accelerate further degradation due to the action of degradation products[39,40,42].

1.3 POLYMER MATRICES

A polymer is composed of repeated units in long chain structures with properties depending on the chemical structure of the repeating unit. Polymers can be naturally occurring, such as cellulose, wool, silk, natural rubber, proteins and DNA, or synthetic. Synthetic plastics are used in a wide range of applications from single-use products and packaging to high-performance load-bearing structures in the automotive, aero and construction industries, including cross-linked thermosets and elastomers (rubber) as well as re-meltable thermoplastic materials, but bioplastics are still less than 1 % by weight of the global plastic production[43]. Apart from using a fossil-based resource for producing synthetic polymers, the waste management and the end-of-life handling are strongly questioning the use of plastics, especially for the short-term use products. After following the concept to refuse or reuse a component, the collected post-consumer waste needs to be increased to avoid littering and increase recycling or energy recovery rates. In 2017, almost 80 % of the globally used polymeric materials ended up in landfills, the environment or the ocean [44].

The polymer matrices used in this study were ethylene-acrylic acid copolymers (EAA) and low density polyethylene (LDPE). Ethylene-acrylic acid is a thermoplastic copolymer consisting of alternating ethylene and acrylic acid sections. EAA was selected as matrix material because it has a lower melting temperature than pure polyethylene and because acrylic acid increase the hydrophilicity, providing a material expected to be more compatible with the cellulose reinforcement, giving a better dispersion and better adhesion between fibre and matrix. The EAA is available with different acrylic acid contents, it is usually available in the form of pellets, but it is also available as an aqueous polymer dispersion. LDPE was selected as a matrix material not only because it is one of the most

common thermoplastic polymers, but also because it has a melting temperature lower than the degradation temperature of the cellulose reinforcement.

1.4 PROCESSING OF CELLULOSE-REINFORCED COMPOSITES

Thermoplastic composites with a cellulose-based reinforcement can be processed by various techniques, but a continuous process is preferred for most applications. The processing method, including mixing, compounding and shaping, will to a great extent determine the final properties of the material by affecting e. g. the dispersion of the reinforcements, degradation and the orientation. Dispersion of the reinforcing elements during processing is important for the mechanical properties of the composite[25,45]. The hydrogen bonds between the cellulose fibres as well as the difference in surface character between the cellulose and the matrix make the dispersion difficult, leading to aggregated fibres with a lower aspect ratio and poorer mechanical properties than a single element. High temperatures, long exposure times and extensive shear forces also affect the degradation behaviour.

Batch-wise production using e.g. solvent casting, dispersion mixing or a micro extruder is commonly applied when nanocellulose is used as reinforcing element. These processes are convenient for use on a laboratory scale but difficult to convert to large-scale industrial compounding[32,36,46], and the feasibility of using conventional melt-processing techniques should be considered[36,47]. The mixing of polymer and CNC in an aqueous dispersion without the application of any additional external force or heat may provide a well dispersed CNC for further mixing processing. After drying these mixtures, compression moulding may be used to shape the composite into a material with properties that cannot be compared with those of materials produced using methods where shear forces are applied[48], e.g. injection moulding or extrusion.

The continuous production of a polymer composite on a large scale involves two steps: mixing of the reinforcing element with the matrix and additional compounding followed by a melt-shaping extrusion or injection moulding. The mixing is important to achieve a good dispersion and avoid aggregates. The degree of dispersion can be improved by applying high shear forces and an elongation flow field, but using compatibilizers or surface grafting of functional groups may also improve both the dispersion and the adhesion between matrix and reinforcement[49]. The shear forces applied during mixing and compounding might lead to an undesired aggregation of the filler, especially if the matrix and reinforcement are incompatible[50,51], but the mixing could possibly be improved by a repeated run of the material through the mixing extruder to increase the amount of shearing but this might also increase the risk of thermal degradation[2,52,53].

Extrusion could be performed using a single-screw (SSE) or twin-screw configuration (TSE), where the material is heated and melted while the screw rotation moves the melt towards

a die. The TSE is expected to provide a better mixing, especially if the screws are co-rotating. Other advantages of TSE are its degassing capacity and the possibility to feed components down stream, which could be beneficial when adding cellulose-based reinforcement sensitive to thermal degradation.

In order to reduce the risk of aggregation of CNC into larger particles, a master-batch approach could be used, the CNC then being mixed with a carrier polymer, compatible with both cellulose and matrix, before being added to the matrix polymer, but it has been shown that liquid feeding and water-assisted extrusion can be a more effective way to reduce the degree of aggregation[36,54,55]. The extent of discoloration has been shown to be reduced by the presence of water in the system[56–58].

Injection moulding is a commonly used technique for producing polymer components with high productivity and little part-to-part variation[59], the material being conveyed by a screw device before injection into a mould. The high pressure and the high elongational flow and high shear fields influence the final properties of the product, and successful injection requires control of the temperature, pressure, time and machine movements[60].

1.5 AIM

The aim of this work has been to seek to replace fossil-based polymeric materials with renewable wood-based materials by using wood-based materials as reinforcement in thermoplastic composites. The specific aim of the project was to improve the mechanical and thermal properties as well as the appearance of the composites and to explore the possibilities of using large-scale production methods for thermoplastic materials. Special attention has been devoted to melt processing by extrusion and injection moulding, to improve the final properties of the composite. A further aim was to explore the possibility of modifying the properties of CNC by surface modification, to enhance its compatibility with the polymer matrix and increase the reinforcing effect of the CNC.

2 MATERIALS

Two different materials have been employed as polymer matrix. The ethylene-acrylic acid copolymer (EAA) was used extensively because it is more hydrophilic in nature than the commonly used polyethylene. Using EAA was expected to increase the compatibility between the hydrophilic CNC and the matrix. The low melting point of EAA was considered beneficial, allowing for melt processing without the risk of excessive thermal degradation of the cellulosic reinforcement. LDPE was also used as a matrix material, it was chosen due to its large availability and commonness, and to its relatively low melting point. Polyethylene can also be of interest from the aspect that suitable bio-based grades are available[61].

2.1 ETHYLENE-ACRYLIC ACID COPOLYMER

The ethylene-acrylic acid copolymer (EAA) dispersion used in Papers I and II was obtained from BIM Kemi AB, Sweden. This grade had an acrylic acid content of 15 %, a melting point of 88 °C, a density of 0.994 g/cm^3 and a melt flow rate of 36 g/10 min (ISO 1133, 190 °C, 2.16 kg) according to the supplier. The dispersion had a solids content of 20 wt.% EAA and pH 9.7.

The EAA pellets used in Papers III and V were an ethylene-acrylic acid copolymer (EAA), Primacor 3540 from Dow Chemical Company, with an acrylic acid content of 7 %. This EAA grade had a number average molecular weight (M_n) of 16100 g/mol, a density of 0.932 g/cm^3, a melting point of 95 °C and a melt flow rate (ISO1133) of 8 g/10 min, according to the supplier.

2.2 LOW DENSITY POLYETHYLENE

The low-density polyethylene (LDPE) grade used in Paper IV was a medical grade obtained from Borealis AG (FT6230) without additives, with a density of 0.913 g/cm^3 and a melt flow rate of 2 g/10 min (ISO 1133). In Paper V, a LDPE grade 19N730 from Ineos Olefins and Polymers was used, with a density of 0.92 g/cm^3, a melting point of 108 °C and a melt flow rate of 8 g/10 min (ISO 1133), all according to the supplier.

2.3 CELLULOSE NANOCRYSTALS

Cellulose nanocrystals (CNC) were used as reinforcement in Papers I, II and V, but the CNC was prepared by different routes. The never-dried CNCs in Papers I and II were obtained by sulphuric-acid-hydrolysis of microcrystalline cellulose (MCC) type Avicel® PH101 with an average particle size of 50 μm, using a procedure described by Hasani et al.[62].

In Paper V, sulphuric-acid-hydrolysed cellulose nanocrystals were obtained as a neutralised (Na^+) spray-dried powder, dispersible in water, from Celluforce, Canada, which was dispersed in water to a dry content of 6-7 wt.%, using an IKA T25 digital Ultra Turrax at a rotational speed of 7400 rpm for 10 min.

2.4 CELLULOSE TISSUE OR FIBRES

Two different kinds of tissue paper made of chemical pulp were used as sources of cellulose fibres, denoted CF in Paper II and CT in Paper IV. The CF in Paper III was a two-layered tissue with 100 % primary fibres from Metsä tissue, Sweden/Finland. This tissue had a sheet grammage of 34 g/m^2 and consisted of 75 % birch fibres and 25 % softwood pulp and was free from any additives. In Paper IV, another two-layered tissue consisting of 75 % short fibres (eucalyptus) and 25 % long fibres (pine) was used; it had a grammage of 34 g/m^2 and is denoted CT.

2.5 THERMOMECHANICAL PULP

The thermomechanical pulp (TMP) originated from spruce and was supplied by Stora Enso, having an average particle length of 1.7 mm and width 20-40 μm.

2.6 ANTIOXIDANT IRGANOX 1010

Irganox 1010 (Pentaerythritol tetrakis(3-(3,5-di-tert-butyl-4-hydroxyphenyl) propionate)), a hindered phenolic primary antioxidant (radical scavenger) (Flick 2004), was used as a thermo-oxidative stabilizer in the durability study in Paper IV.

3 EXPERIMENTAL

In-depth descriptions of the techniques and the conditions used can be found in the appended Papers.

3.1 SURFACE GRAFTING OF CNC

The CNC prepared as described in section 2.1 was modified following three different routes to graft chemical groups onto the cellulose surface.

In Paper I, the procedure outlined by Chattopadhyay et al. [63] was followed, using methylated azetidinium salts to react with sulphate groups on the CNC to graft three different chemical groups onto the cellulose surface: N-morpholino-3-methoxyazetidinium, N,N-diallyl-3-methoxyazetidinium and N,N-dihexyl-3-methoxyazetidinium. For the production of composites (Paper II), the methylation was omitted, resulting in a hydroxy functionality instead. No significant differences were observed in the performance of the surface-treated CNC due to this omission, but it made the modification procedure more straightforward. The surface modifications are denoted in the following as MorphCNC, diAllylCNC and diHexylCNC respectively, regardless of reaction route used. The molecular structure of the three different groups and the three different reagent routes are shown in Figure 1. The synthesis of the azetidinium salts is described in detail in Papers I and II.

Hasani et al. [62] have shown that the dimensions of the CNC did not change significantly as a result of this type of surface grafting. The increase in weight of the CNC as a result of the surface modification was considered to be negligible[64].

Due to the promising results obtained, it was decided to focus the upscaling of the process on the diallyl-modification. In Paper V, the diallyl-modification was performed on the CNC from CelluForce, as described in section 2.1. Due to difficulties in producing large quantities of high-quality azetidinium salts, the modification was carried out using a cyclic carbonate reagent (4-((diallylamino)methyl)-1,3-dioxolan-2-one). The synthesis of the carbonate reagent was performed as described in Paper V according to a two-step reaction scheme, outlined by Reddy[65] and Parzuchowski[66].

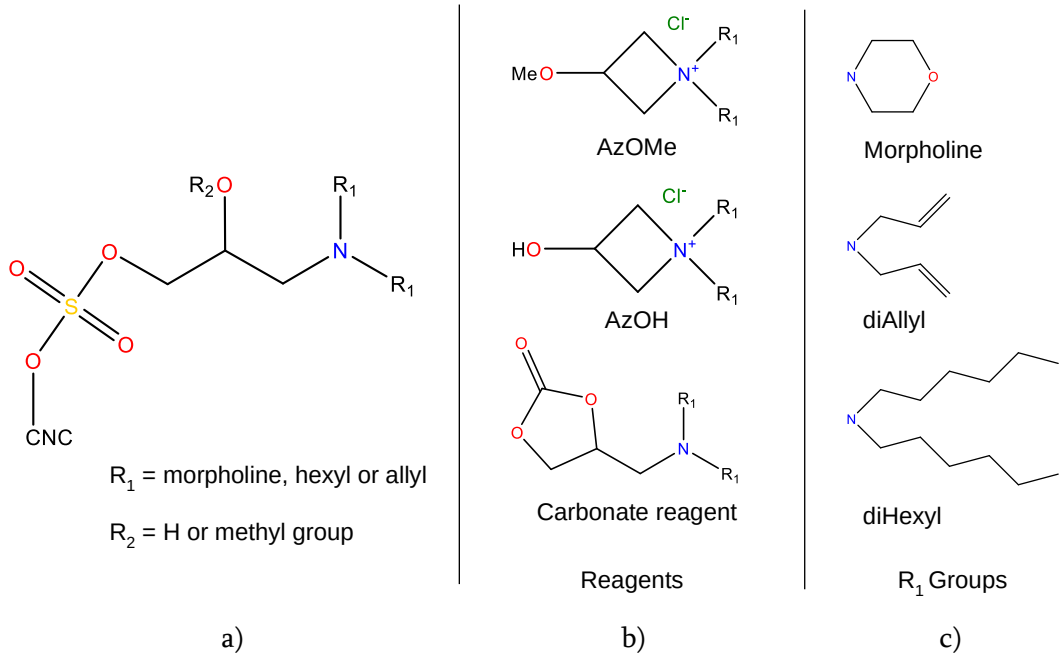

Figure 1: The molecular structures of the surface modifications. a) schematic view of the surface grafted CNC. The surface grafting can be achieved by using any of the three reagents in b), resulting in a R_2 of Methyl when using AzOMe and H as R_2 when using AzOH or carbonate reagent. c) schematic outline of the three different grafting groups, R_1.

3.2 Manufacturing processes

The processing techniques used in Papers II-V are listed in Table 1.

Table 1: Compounding and shaping techniques used in Paper II-V

Paper	Mixing and compounding		Shaping		
	Dispersion mixing	Twin-screw extrusion	Compression moulding	Single-screw extrusion	Injection moulding
II	X		X		
III		X			X
IV		X		X	
V		X			X

3.2.1 Dispersion mixing

Aqueous dispersions of CNC and EAA were blended to give 0.1, 1 and 10 wt.% CNC concentration levels in the composite materials with both surface-treated CNC and unmodified CNC (Paper II). An IKA T25 digital Ultra Turrax was used for 6 minutes at 7400 rpm to ensure thorough mixing of the components. The aqueous dispersions were then poured onto large plates and allowed to dry in air at room temperature for approximately one week, giving approximately 20 g of thin flakes of a mixture of polymer and CNC.

3.2.2 Melt mixing and compounding by twin-screw extrusion

In Paper V, a co-rotating, Werner & Pfleiderer ZSK 30 M9/2 (Stuttgart, Germany) twin-screw extruder (TSE) was used for continuous production in a two-step process with an initial water-assisted melt mixing, followed by a second homogenising (compounding) extrusion. The CNC dispersion with unmodified or diallyl-modified CNC from Celluforce, prepared as describe in section 2.1, was added to the hopper together with the polymer pellets. A peristaltic pump Heidolph SP standard, PD 5001 (Schwabach, Germany) was employed for the less viscous unmodified CNC but a syringe was used for the more viscous diallyl-modified CNC dispersion. The feeding rates were adjusted to give a CNC content of 10 wt.% in the composites. The water-assisted extrusion was carried out using the mixing screw configuration design (MS) at 50 rpm whereas the second compounding step was performed using the compounding screw (CS) configuration at 70 rpm. The two screw configurations (MS and CS) are shown in Figure 2. The material was compounded twice in the TSE and pelletized after each cycle before the final shaping step. The TSE had a screw diameter of 30 mm, a screw length of 971 mm, five heating zones along the cylinder and one heating zone at the die. The temperature profile from the hopper to the die for the first pass (mixing step) was 80-90-130-130-120-120 °C and 120-140-200-200-170-170 °C for the second pass (compounding step).

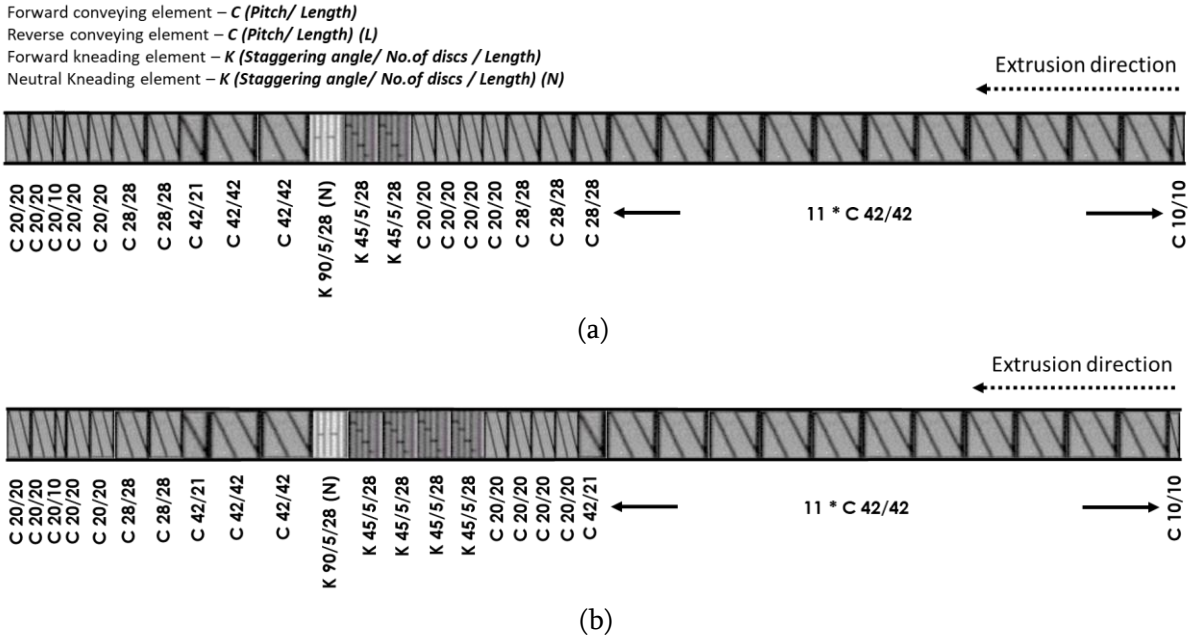

Figure 2: The two screw configurations used for water-assisted mixing and compounding; (a) Mixing screw (MS) and (b) Compounding screw (CS)

In Papers III and IV, the composites containing TMP or CT/CF were produced by mixing and compounding using the TSE described above but with the cellulosic compound being fed into the polymer melt in the middle section of the screw, see Figure 3. The TMP and CT/CF were dried at 75 °C for at least three days before mixing.

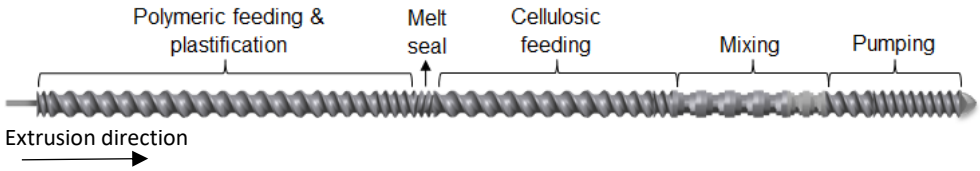

Figure 3: The screw configurations used for mixing and compounding of TMP or CT/CF composites, from the inlet to the die

The temperature profile for the twin-screw extrusions for the compounds with LDPE as the matrix material in Paper IV was 120-170-180-180-190-190 °C. The screw speed for the first mixing, varied between 18 and 50 rpm. The screw speed was selected to give a material flow rate of 45 and 35 g/min to achieve a reinforcement content of 20 and 5 wt.% respectively. In the second TSE compounding, the screw speed was kept constant at 45 rpm in all cases.

The CF-containing composites with EAA as matrix material (Paper III) were compounded with a lower temperature profile from hopper to die: 100-130-140-140-150-150 °C. The screw speed was set to 96 rpm and the cellulosic tissue feed rate was balanced in relation to the screw speed in order to obtain a cellulose content of 20 wt.% in the composite.

3.2.3 Shaping by compression moulding, single screw extrusion and injection moulding

CNC composite materials were produced at a small scale by compression moulding 12 g of the dried flakes of the EAA and CNC in a hydraulic press (Buscher-Guyer KHL 100, Switzerland) to give square plates 100 x 100 mm^2 in size and about 1 mm thick. The compression moulding was carried out at 105 °C and with a maximum pressure of 500 bar, for approximately 5 min. A detailed description is given in Paper II.

The large-scale production of CNC composites (Paper V) and of CT-containing composites (Paper III) was carried out using an injection moulding machine type Arburg Allrounder 221M-250-55 (Austria), producing square plates with dimensions of 64 x 64 x 1.5 mm^3. The sprue from the cylinder nozzle to the cavity diverged from a diameter of 4 mm to a diameter of 7 mm along the sprue length of 54 mm, followed by an 18 mm long runner with a cross section of 40 mm^2 and a rectangular cavity gate having a 8 x 1.5 mm^2 cross section and a land length of 1 mm. The mould temperature was 25 °C and the injection pressure 75 MPa. The holding pressure was 80 MPa and the backpressure 1.5 MPa. The circumferential screw speed was set to 20 m/min. The injection speed was 50 cm^3/s when filling the sprue, and this was reduced to 20 cm^3/s when filling the mould cavity. For the CNC composites in Paper V, the temperature profile from the hopper to the nozzle was 110-150-150-170-170 °C and the injection moulding cycle time was 45 s, including 10 s holding time and 30 s cooling time. The CF-reinforced composites in Paper III were produced with three different temperature profiles, with increasing temperature along the barrel to arrive at 170, 200 and 230 °C respectively in the two last heating zones before the nozzle. The materials were

denoted according to the temperature in the two last zones, e.g. CF170. In each injection moulding series, the first 20 samples were discarded before the process was considered stable.

A Brabender 19/25D single-screw extruder (SSE) was used to produce thin strips of TMP-reinforced or CT-reinforced LDPE for accelerated ageing studies (Paper IV). A Maillefer barrier type screw with a diameter of 19 mm and a length of 475 mm, and with a 2.5:1 compression ratio and a final distributive mixing section was used for the SSE. The temperature profile along the barrel was 120-170-180-190 °C and the screw speed was 25 rpm. A ribbon die head, 50 mm wide and 0.5 mm high, together with a Brabender Univex flat film take-off unit was used to give the final shape and to stretch the material into flat homogeneous strips with a thickness of 0.55 ± 0.05 mm.

3.3 CHARACTERIZATION

3.3.1 Thermal stability and appearance

The thermal stability of the composite materials was studied by thermogravimetric analysis using a TGA/DSC 3 + Star system (Mettler Toledo, Switzerland). The samples were heated from 25 °C to 500 °C at a rate of 5 °C/min or 10 °C/min in a nitrogen atmosphere. The mass loss and onset temperature for degradation was calculated using the Mettler Toledo STARe evaluation software.

The thermal transitions and crystallinity were assessed by differential scanning calorimetry, DSC, using a Perkin-Elmer DSC7 or a Mettler Toledo DSC2 calorimeter equipped with a HSS7 sensor and a TC-125MT intercooler. The endotherms were recorded with increasing temperature from 25 to 160 °C at a scan rate of 10 °C/min in a nitrogen atmosphere. The Mettler-Toledo DSC 2 was also used to determine the oxidation induction time *(OIT)* of the composite materials subjected to accelerated thermo-oxidative ageing in accordance with the ISO 11357-6 and ISO11357-1 standards (Paper IV).

The colour of the composite materials was determined using a Datacolor 600 spectrophotometer with a 9 mm diameter opening and a d/8° measurement. The colour was expressed in the 1976 CIELAB system ("ISO/CIE 11664-4:2019," 2019) with coordinates L^* (lightness), a^* (red-green) and b^* (yellow-blue). The gloss was measured with a Konica Minolta Uni Gloss 60Plus or a BYK Gardner-micro-TRI-gloss with an angle of incidence of 60 ° at room temperature. The surface topography of the injection-moulded samples in Paper III was characterized using an S Neox optical instrument from Sensofar (Spain) according to the ISO 25178 standard using MountainsMap ver. 7.4.8341 software from Digital Surf (France).

The composites containing the different surface-modified CNCs in Paper II were examined visually using a heat-gradient Kopfler Bench, to compare discoloration effects and hence the initiation temperatures for thermal degradation. Small samples of the composites of both surface-treated and untreated 10 wt.% CNC and a reference sample with pure EAA, were heated at 120, 130, 140, 150 and 160 °C for 8 minutes.

3.3.2 Accelerated thermo-oxidative ageing

The strips of LDPE reinforced with TMP/CT (Paper IV) were subjected to accelerated thermo-oxidative ageing at 90 °C in a Termaks TS8430 laboratory heat chamber. Eight strips of each material were conditioned for at least 48 hours at 23 ± 2 °C and 50 ± 5 % RH, before being hung well separated in the heat chamber. The oxidation induction time (*OIT*) and mechanical properties were continuously determined during the first 31 days (744 h) of ageing. At this point, OIT of all the composites without added antioxidant (AO) was shorter than 5 min, and the resistance to thermal oxidation was considered to be exhausted. The accelerated ageing of the composites containing added AO was continued, with sampling up to 3528 h (147 days). FTIR spectroscopy was performed with a Thermo Fisher Scientific Nicolet iS50 FT-IR in the attenuated total reflection (ATR) mode to identify the functional groups present on the surface of the samples, and thus the level of degradation products.

3.3.3 Rheological properties

The rheological properties of the aqueous CNC dispersions (Paper I) and the composite materials (Paper V) were assessed using an Anton Paar MCR 702 Rheometer (Graz, Austria). For the aqueous dispersions, the measurements were performed at 25 °C with a cone-plate configuration with a diameter 50 mm and cone-plate angle 1.991°. The steady-state shear viscosity was determined when the shear rate was varied between 1 and 1000 s^{-1}. The dynamic-mechanical properties were measured on the aqueous dispersions during a strain-sweep at 1 Hz, and the storage modulus *G'* and loss modulus *G"* were assessed as functions of the shear strain amplitude.

The same equipment was used to perform small-amplitude oscillatory shear tests (SAOS) on the injection moulded CNC composites in Paper V. Disk-shaped samples were analysed using a parallel plate geometry (15 mm plate diameter) at 170 °C and the rheological properties of the composites were found to be stable for more than 50 minutes. The thermal degradation during the rheological measurements was assumed to be negligible. In the SAOS experiments, the linear viscoelastic region was assessed using a strain sweep from 1 to 100 % at a constant angular frequency of 1 s^{-1}, and angular frequency sweeps in the range of 0.08–200 s^{-1} were performed at strain amplitudes of 0.04 - 0.7 %.

The shear viscosity of the 10 wt.% CNC composite melts was determined as a function of the shear rate using a capillary viscometer in Paper V (Göttfert Rheograph 2002, Germany).

Two cylindrical capillaries of different length (10 and 20 mm) but with the same diameter (1mm) were used to estimate the pressure entrance losses (Bagley correction of the applied pressure). A 500 bar pressure transducer (Dynisco, USA) was used to record the pressure applied when the melt was pushed through the capillary at different piston speed, which was varied between 0.05 and 2 mm/s, corresponding to shear rates of 58 to 2300 s^{-1}. The measured shear rates were subjected to the Rabinowitsch-correction. The shear viscosities were determined at a melt temperature of 170 °C.

3.3.4 Characterization of surface grafting

To ensure that the surface grafting was successful, a number of characterization methods were applied to the surface-treated CNC. The methods are described in detail in Papers I, II and V.

The ζ-potential of the surface-grafted CNC was measured using a Zetasizer Nano ZS (Malvern Instruments, UK) based on the Laser Dopple Velocimetry technique. The measurements were made at 25 °C using DTS1070 disposable folded capillary cells, with a 50 mW diode-pumped solid-state laser with a wavelength of 532 nm.

The sulphate half ester content was determined using conductometric titration. Typically, a sample volume of 75-100 ml was prepared, containing around 0.1 g CNCs (dry weight). The titrations were either done manually by adding 0.1-1 mL aliquots 10 mM NaOH, in 30-60 s intervals until sufficiently many data points were collected after the equivalence point, monitoring the conductivity with a conductometer (SevenCompact, Mettler-Toledo or Eutech Instruments) or using an automated titrator set-up (Mettler-Toledo). For the automated titrations 0.1 mL aliquots 10 mM standardised NaOH was added in 50-70 steps with 30-60 s intervals.

Fourier-Transform Infrared (FTIR) spectroscopy was performed on either freeze-dried CNC samples pressed into pellets with potassium bromide, or on dried CNC films using ATR-FTIR. The spectra were recorded from 4000 to 400 cm^{-1} and 32 scans were collected.

3.4 MECHANICAL PROPERTIES

3.4.1 Tensile properties

Tensile properties were measured using a Zwick/Z2.5 tensile tester with a 500 N load cell for all composite materials except the composites subjected to accelerated ageing in Paper IV, where an Instron 5984 tensile tester equipped with a video extensometer and a load cell of 500 N was used. Test bars with a gauge length of 40 or 20 mm were cut and conditioned at 50 ± 5 % relative humidity and 23 ± 2 °C for at least four days prior to the tensile tests. The tensile properties were measured at 23 ± 2 °C with a strain rate of $2.5 \cdot 10^{-3}$ s^{-1} (6 mm/min)

except for the materials tested in the Instron 5984 video extensometer where a method employing four ramps where used. A detailed description is given in Paper IV.

3.4.2 Dynamic-mechanical analysis

A Rheometrics RSA II was used to measure the dynamic-mechanical properties of the materials. Samples were pre-strained to a strain of 0.13-0.15 % and a sinusoidal deformation was then superimposed at a constant temperature of 23 °C. The storage modulus, loss modulus and mechanical loss factor data of the materials were used to discuss the adhesion and stability of the interphase between the matrix and the reinforcement.

4 SUMMARY OF RESULTS

The results are here divided into; manufacturing processes, characterization and mechanical properties. The findings from the initial analysis of the surface grafted CNC in Paper I and the further developments in Papers II and V are presented together with the results relating to TMP- and CF/CT-reinforced composites in Papers III and IV.

4.1 MANUFACTURING PROCESSES

The surface grafting was performed using methoxyazetidinium salts (Paper I), hydroxyazetidinium salts (Paper II) or a carbonate reagent (Paper V). In the upscaling of the process in Paper V, the surface grafting process had been further studied and carbonyl groups were used instead of azetidinium salts, which are difficult to produce on a large scale with high purity. The surface grafting of CNC was considered to be successful on the basis of the results of TGA, FTIR and conductometric titration. Further details of the surface grafting are given in section 4.2.5 and in Papers I, II and V.

In Paper I, the aqueous dispersions of CNC were successfully modified with three surface modification groups; Morph, diHexyl and diallyl (Figure 1c). CNC composites were produced on a small-scale at 0.1, 1 and 10 wt.% CNC content by mixing the modified CNC and dispersions followed by drying to obtain well-dispersed CNC in the composite materials[67]. These compounds were compression moulded into plaques, as described in Paper II. Figure 4. show the appearance of the 10 wt.% CNC samples with the three different modifications. Neither the CNC modified with diHexyl nor that modified with diAllyl showed any visible aggregates or discoloration and the transparency was the same as that of the neat EAA matrix and of the composite with unmodified CNC reinforced up to 10 wt.%. The EAA15-10 % MorphCNC composite exhibited a more yellowish appearance and somewhat more visible defects. The discoloration of the EAA15-10 % MorphCNC was not further investigated, but there are reports of the influence of amine structure on the yellowing.[68,69]

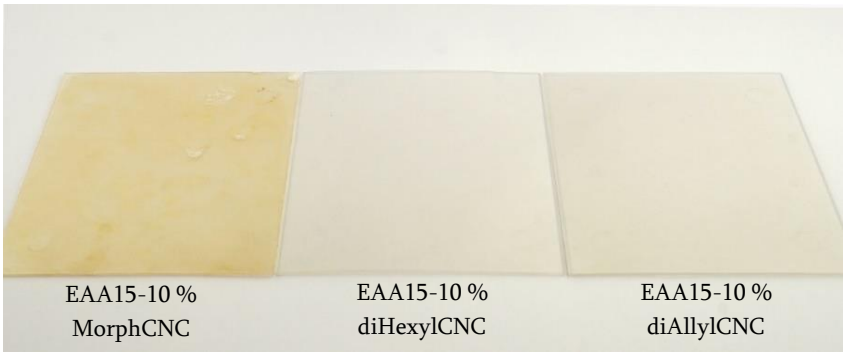

Figure 4: Dispersion-mixed, air-dried and compression-moulded EAA15 composites with 10 wt.% surface modified CNC, from the left; MorphCNC, diHexylCNC and diAllylCNC

To scale-up the production of CNC composites, 3 kg batches of 10 wt.% CNC (diallyl modified and unmodified) reinforced EAA or LDPE were successfully produced using a wet mixing process with TSE followed by injection moulding. This led to a change in transparency and colour as can be seen in Figure 5. Small darker entities, indicating aggregates of CNC in the material were also observed. This was more pronounced in the EAA7 samples and the colour difference was greater when the surface-treated CNC was added to the EAA7 matrix.

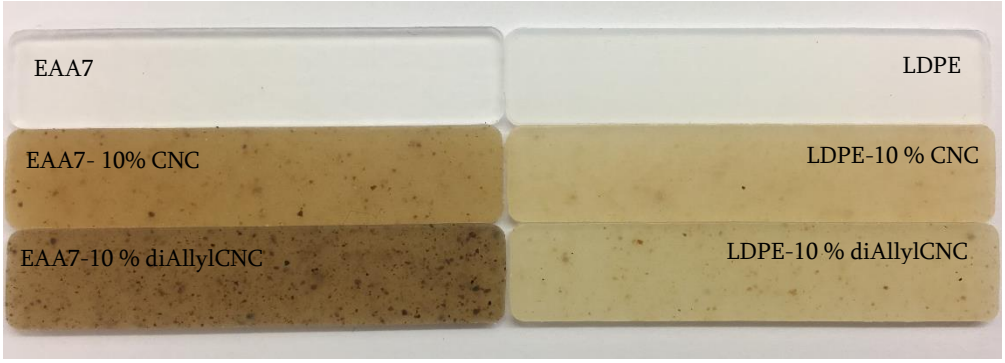

Figure 5: TSE-mixed, injection-moulded composites with 10 wt.% CNC, compounded in 3 kg batches by wet-mixing in TSE

Thermomechanical pulp (TMP) or cellulose tissue (CT or CF) was successfully compounded into the polymer melt using the twin-screw extruder to feed the reinforcement into the polymer melt, and a second TSE was found to greatly improve the homogeneity of the composite compounds[2,52,53,70]. The compounded materials were injection-moulded into plaques at different processing temperatures (Paper III) or single-screw extruded into strips and subjected to accelerated thermo-oxidative ageing (Paper IV).

Figure 6 shows the injection-moulded plaques of 20 wt.% cellulose-fibre-reinforced EAA (CF) and neat EAA, processed at different temperatures. The temperature had a marked influence on the colour of the cellulose-containing plates, causing a yellowing already at a melt temperature of 170 °C and becoming darker with increasing melt temperature. The appearance of the unfilled EAA, on the other hand, did not seem to be affected by the processing temperature, the transparency was preserved regardless of the melt temperature. All the plaques were visually quite homogeneous, indicating that the cellulose fibres were successfully dispersed using the adopted procedure.

The single-screw-extruded strips reinforced with 5 or 20 wt.% cellulose tissue (CT) or thermo mechanical pulp (TMP) are shown in Figure 7. There is no significant difference in colour between the samples without (upper row) and with antioxidant (lower row). The addition of TMP gave the composite a light brown colour whereas the addition of CT resulted in a light-yellow appearance. There was no significant filler aggregation in either the TMP-containing or the CT-containing samples.

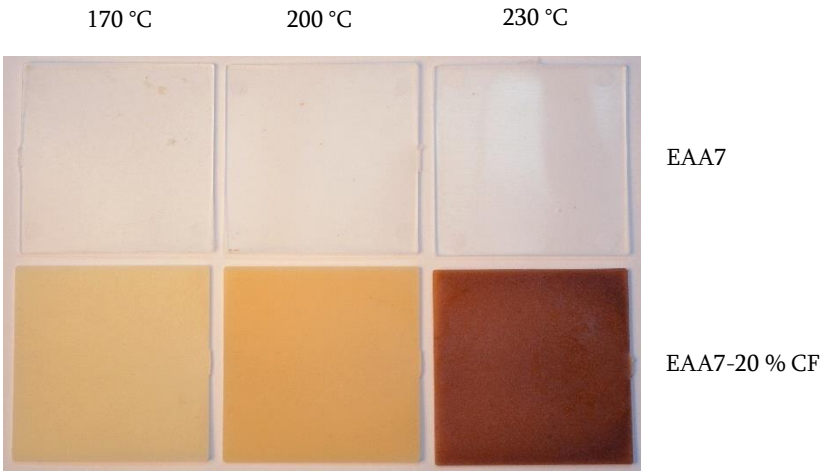

Figure 6: Injection-moulded cellulose-reinforced composites produced at three different processing temperatures and the unfilled matrix material treated at the same temperatures

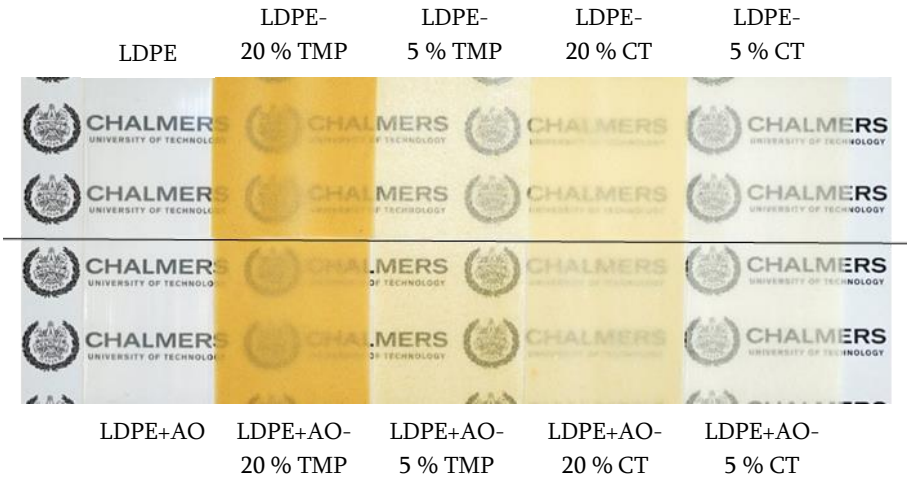

Figure 7: Single-screw-extruded strips of LDPE reinforced with 5 or 20 wt.% cellulose or thermomechanical pulp and the neat LDPE, where the top row are the materials without antioxidant and the lower row are the materials with antioxidant

4.2 CHARACTERIZATION

4.2.1 Thermal stability

The thermal stability was investigated mainly by thermogravimetric analysis. The onset temperature of thermal degradation and the crystallinity of the CNC composites are listed in Table 2. The surface-grafted CNC had an onset temperature about 100 °C higher than that of the unmodified CNC, as shown in Figure 8. This can be attributed to the conjugation with the sulphate half ester, preventing the catalysed degradation seen in the unmodified material [34,71].

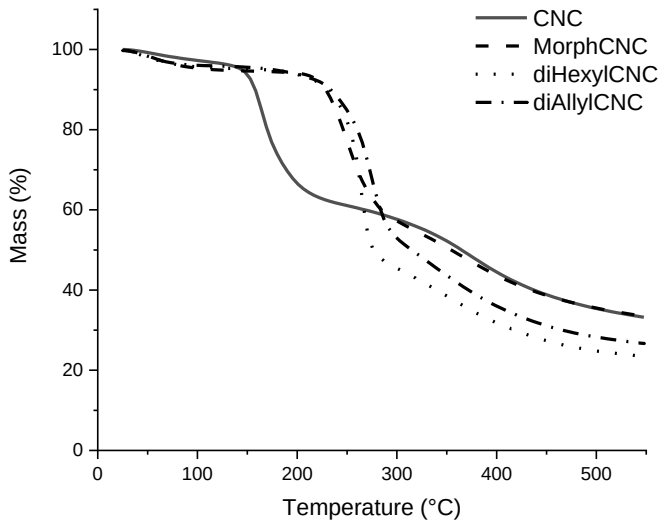

Figure 8: Thermogravimetric curves showing the mass of the unmodified CNC and of the azetidinium-grafted CNC (before mixing with polymer) as a function of temperature

When CNC was incorporated into the EAA15 matrix by dispersion mixing and compression moulding, however, the functional groups grafted onto the CNC did not improve the thermal stability of these composites. Figure 9a shows the appearance of the composites containing 10 wt.% CNC after exposure to (from right to left) 120, 130, 140, 150 and 160 °C for 8 minutes. At 150 °C, the colour started to change and at 160 °C all the samples were brown. No significant difference between the composites was detected, indicating that the functional groups grafted onto the CNC did not increase the thermal stability of these EAA-based composites. With unfilled EAA, there was no colour change at all up to 160 °C, and the samples remained transparent. The TGA results (in Figure 9b) confirmed that the thermal degradation of the composites began at ca 150 °C. This was somewhat surprizing since the TGA of the modified CNC showed thermal stability up to ca 250 °C, as shown in Figure 8. It is well established that sulphates act as good leaving groups in the presence of a nucleophile such as hydroxide and carboxylate which is abundant at pH 9.7 (the pH-level of the EAA-dispersion), so the azetidinium groups on the sulphate diesters are cleaved by the carboxylates of the EAA matrix generating sulphate half-esters that have a lower thermal stability. At neutral pH, the carboxylate is in the carboxylic acid form and it is then less prone to react with the sulphate diester, and no degradation at 150 °C is observed. The pH-neutral composite containing 10 wt.% diAllylCNC did not show any change in colour up to 160 °C, as shown in Figure 9a.

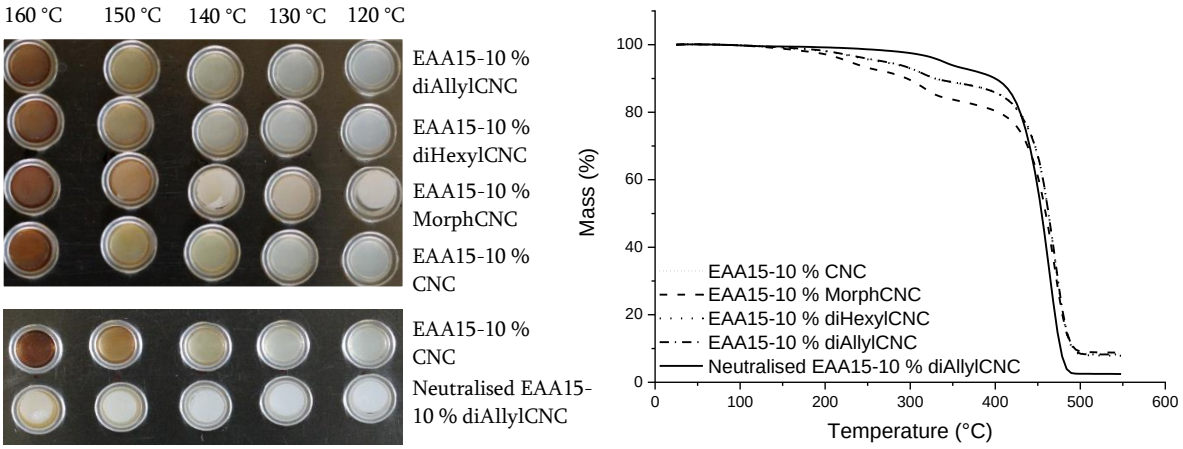

Figure 9: a) Upper photograph: The composites containing 10 wt.% CNC after exposure to (from right to left) 120, 130, 140, 150 and 160 °C for 8 minutes. Lower photograph: The untreated CNC composite and the sample produced under neutralised processing conditions, after exposure to (from right to left) 120, 130, 140, 150 and 160 °C for 8 minutes. b) Thermogravimetric curves showing the mass of the composites containing unmodified CNC, the azetidinium-grafted CNC and a model sample produced under neutralised conditions as a function of temperature

Figure 10 shows that in the case of the 10 wt.% composites produced by wet mixing of TSE and injection-moulding the composites reinforced with unmodified CNC exhibited a greater thermal stability (270 °C) than those reinforced with modified CNC (240 °C).

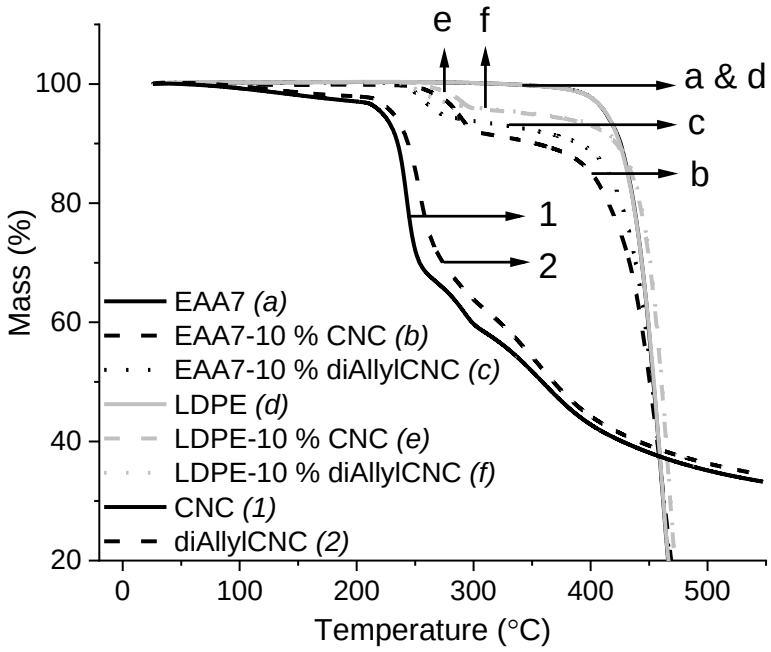

Figure 10: Thermogravimetric curves showing the mass of the neat CNC; unmodified and modified, the polymer matrices and composites as a function of temperature

Although the EAA7-CNC composite was more discoloured, the samples had a similar degradation temperature profile. The degradation temperature was higher with the unmodified CNC from CelluForce than with the unmodified CNC used in Papers I and II, because the CelluForce CNC had Na^+ as counterion. The darkening of the diAllyl-modified composite with EAA7, Figure 5., was assessed to be because the alkali content of the EAA7 pellets initiated the degradation.

The TGA measurements on the CT/CF- or TMP-reinforced composites showed no significant differences in thermal stability and these materials were studied more with regard to their appearance; colour, gloss and surface roughness. No significant differences in crystallinity or melting point between any of the composite materials and the corresponding neat matrices were observed.

Table 2: Summary of crystallinity and onset temperature of thermal degradation of the composites with CNC

Comment	Material	Crystallinity (%)	T_{onset} (°C)
Dried CNC from MCC, AzOMe-modified	CNC from MCC	-	157
	MorphCNC	-	250
	diHexylCNC	-	246
	diAllylCNC	-	242
Dried CNC from CelluForce	CNC CelluForce	-	236
	diAllylCNC (Carbonate)	-	238
	diAllylCNC (hydroxyazetidinium)	-	263
CNC from MCC, AzOH-modified, dispersion-mixed, air-dried, compression-moulded (Paper II)	EAA15	17	430
	EAA15-10 % CNC	18	235
	EAA15-10 % MorphCNC	18	224
	EAA15-10 % diAllylCNC	15	247
	EAA15-10 % diHexylCNC	19	247
	Neutralised EAA15-10 % diAllylCNC	-	301
CelluForce CNC, AzOH-modified, produced as in Paper II (reference)	EAA7-10 % CNC	-	239
	EAA7-10 % diAllylCNC	-	239
	EAA15-10 % CNC	-	249
	EAA15-10 % diAllylCNC	-	237
	EAA15-10 % diAllylCNC (Carbonate modified)	-	227
CelluForce CNC, Carbonate-modified, wet-mixed, TSE, injection-moulded (Paper V)	EAA7	16	430
	EAA7-10 % CNC	16	265
	EAA7-10 % diAllylCNC	14	239
	LDPE	22	441
	LDPE-10 % CNC	21	272
	LDPE-10 % diAllylCNC	20	238

4.2.2 Appearance

Table 3. summarizes the colour and gloss results for the injection moulded 10 wt.% CNC composites (Figure 5). A clear reduction in lightness (L^*) was noted for both the EAA7 and the LDPE composites compared to the unfilled matrix, particularly in the EAA7 composite. All the reinforced samples were significantly more yellow than the neat matrices and the addition of CNC to EAA7 resulted in a somewhat increased redness. All the composites exhibited similar gloss values. The slight decrease relative to the unfilled material was probably due to the rougher surface caused by the addition of the reinforcing element.

The temperature affected the colour of the 20 wt.% cellulose fibre reinforced EAA (Figure 6). These specimens developed a yellowish appearance already at 170 °C and became darker with increasing process temperature. The visual appearance was confirmed by the values in Table 3., where the L^*-value decreased markedly and the b^*-value increased in the composite processed at higher temperatures. The specimen processed at 230 °C exhibited a quite strong increase in a^*-value compared to those processed at lower temperatures.

Table 3: The CIELAB colour coordinates and gloss values of the composite materials and unfilled polymer matrices injection-moulded into plaques

	L^*	a^*	b^*	Gloss (%)
EAA7	84.0	2.5	-3.5	26.9
EAA7-10 % CNC	58.9	4.7	21.3	19.9
EAA7-10 % diAllylCNC	52.2	6.0	19.2	21.7
LDPE	77.3	2.6	-4.6	16.7
LDPE-10 % CNC	68.2	2.2	13.2	22.8
LDPE-10 % diAllylCNC	69.1	0,9	13.2	26.1
EAA7 170	84.7	2.36	-3.85	12.8
EAA7 200	85.3	2.44	-3.42	15.3
EAA7 230	85.8	2.46	-3.57	15.9
EAA7-20 % CF 170	72.8	-1.39	6.17	7.9
EAA7-20 % CF 200	68.0	-1.97	26.63	7.6
EAA7-20 % CF 230	43.3	14.31	23.34	6.3

The composites with either TMP or CT with 5 or 20 wt.% reinforcement described in Paper IV also displayed a clear colour difference and a reduction in transparency compared to the neat LDPE matrix. The specimens reinforced with TMP were yellower than those reinforced with the cellulose tissue. In Paper III, the surface roughness of the 20 wt.% cellulose fibre reinforced composites was examined. A clear difference in surface roughness could be observed comparing the neat matrix and the composite specimens, where the composites had a rougher surface as can be seen in Figure 11. These results were supported by the lower gloss values for the composite materials, in which cellulose fibres and CNC were used as reinforcing element (Table 3). The process temperature did not seem to affect the surface roughness of the pure EAA but the composite surfaces became less rough with

increasing process temperatures, probably due to a better replication of the relatively smooth mould surface[72].

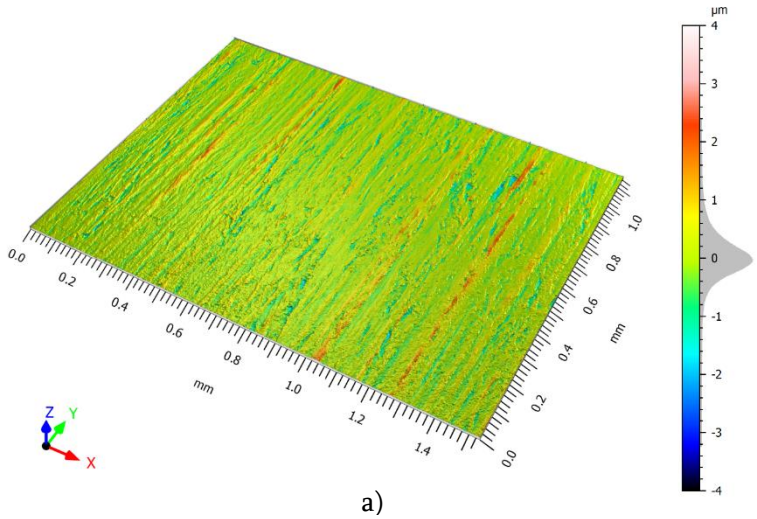

a)

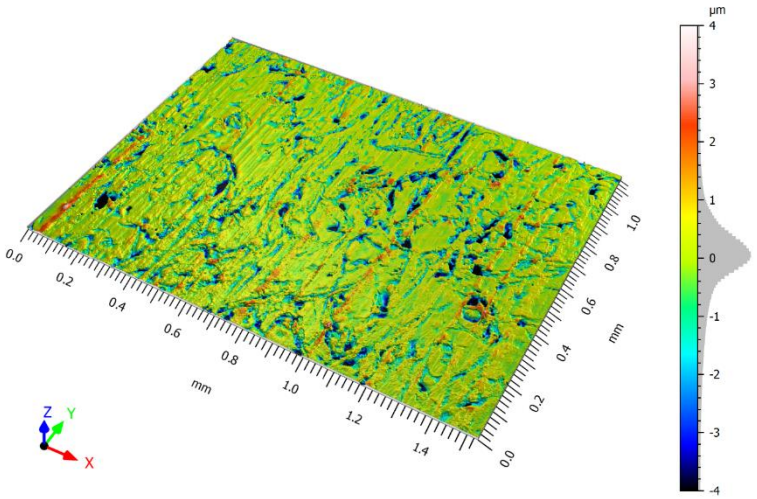

b)

Figure 11: Surface roughness of a) EAA7 170 and b) EAA7 - 20 % CF 170

4.2.3 Thermo-oxidation

The thermo-oxidative behaviour of the TMP or CT reinforced composites was characterized by determining the oxidation induction time (*OIT*) after accelerated ageing at 90 °C. Figure 12 and Table 4 show the *OIT* of the materials as a function of ageing time. Most of the materials without added antioxidant exhibited an *OIT* of ca 0.5 min, regardless of ageing time, indicating an insignificant resistance to thermal degradation (Figure 12a). The only exception was the LDPE-20 % TMP sample which had an initial *OIT* of 6.8 ± 3.1 min before ageing, suggesting that the addition of 20 wt.% TMP to the LDPE matrix might delay the thermo-oxidation, possibly because the lignin acted as an antioxidant [41,73–75]. After ageing at 90 °C for 144 h, the *OIT* of the LDPE-20 % TMP also decreased to 0.5 min, indicating that the ageing had consumed the stabilizing effect of the added TMP.

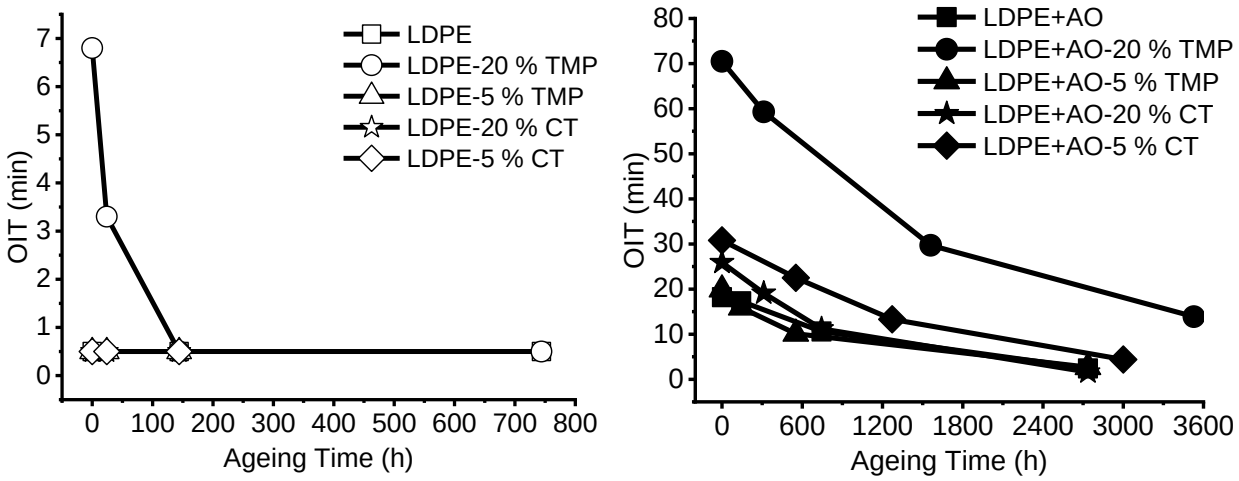

a) b)

Figure 12: The oxidation induction time (OIT) after different ageing times for samples a) without and b) with added antioxidant

The *OIT* of the samples with added antioxidant are shown in Figure 12b, indicating a much stronger resistance to thermo-oxidation for all samples. The LDPE+AO-20 % TMP had the greatest resistance, with an *OIT* of 13.9 min after 3528 h accelerated ageing. The ageing time for each material to reach an *OIT* value shorter than 5 min, is given in Table 4.

Table 4: Oxidation induction time (OIT) of all samples prior to ageing and the aging time to reach an insignificant resistance to thermal degradation, with an OIT shorter than 5 min. Standard deviations in parentheses

	OIT (min)				
Material	0 h	24h	2736 h	3000 h	3528 h
LDPE	0.4 (0.05)				
LDPE-20 % TMP	6.8 (3.1)	3.3 (1.3)			
LDPE-5 % TMP	0.5 (0.04)				
LDPE-20 % CT	0.5 (0.03)				
LDPE-5 % CT	0.5 (0.01)				
LDPE+AO	18.2 (1.7)		2.4 (1.1)		
LDPE+AO-20 % TMP	70.5 (5.0)				13.9 (1.3)
LDPE+AO-5 % TMP	19.9 (2.7)		2.7 (0.5)		
LDPE+AO-20 % CT	25.9 (1.4)		1.6 (0.2)		
LDPE+AO-5 % CT	30.8 (4.6)			4.4 (1.5)	

The addition of cellulose tissue (CT) had less effect than the addition of TMP on the *OIT*, but it nevertheless increased the resistance to oxidation relative to the LDPE-AO matrix. This stabilizing effect of a combination of TMP and a commercial AO has been reported previously by Gregorová et al. [73]. Figure 12a shows that the addition of 20 wt.% TMP significantly increased the OIT of LDPE, but the increase was even greater in combination with AO, as shown in Figure 12b.

The formation of carbonyl groups (C=O), which is an indication of thermo-oxidation, was assessed using FTIR-spectroscopy. The full FTIR-ATR spectra are given in Paper IV. There was no great increase in absorbance in the hydroxyl group (-OH) region (3000-3500 cm-1) [76] after the ageing, which implies that the degradation led mainly to an increase in the carbonyl group absorbance. Figure 13 provides a more detailed overview of the carbonyl bands (1680-1800 cm^{-1}) after several ageing times for the unfilled LDPE and for the composites containing 20 wt.% TMP or CT, with and without AO. This enhanced peak height after ageing of the materials without added AO indicates the presence of acid, ester and lactone groups [76–79]. The increase in peak height for the samples containing AO was much smaller and appeared only after much longer ageing times.

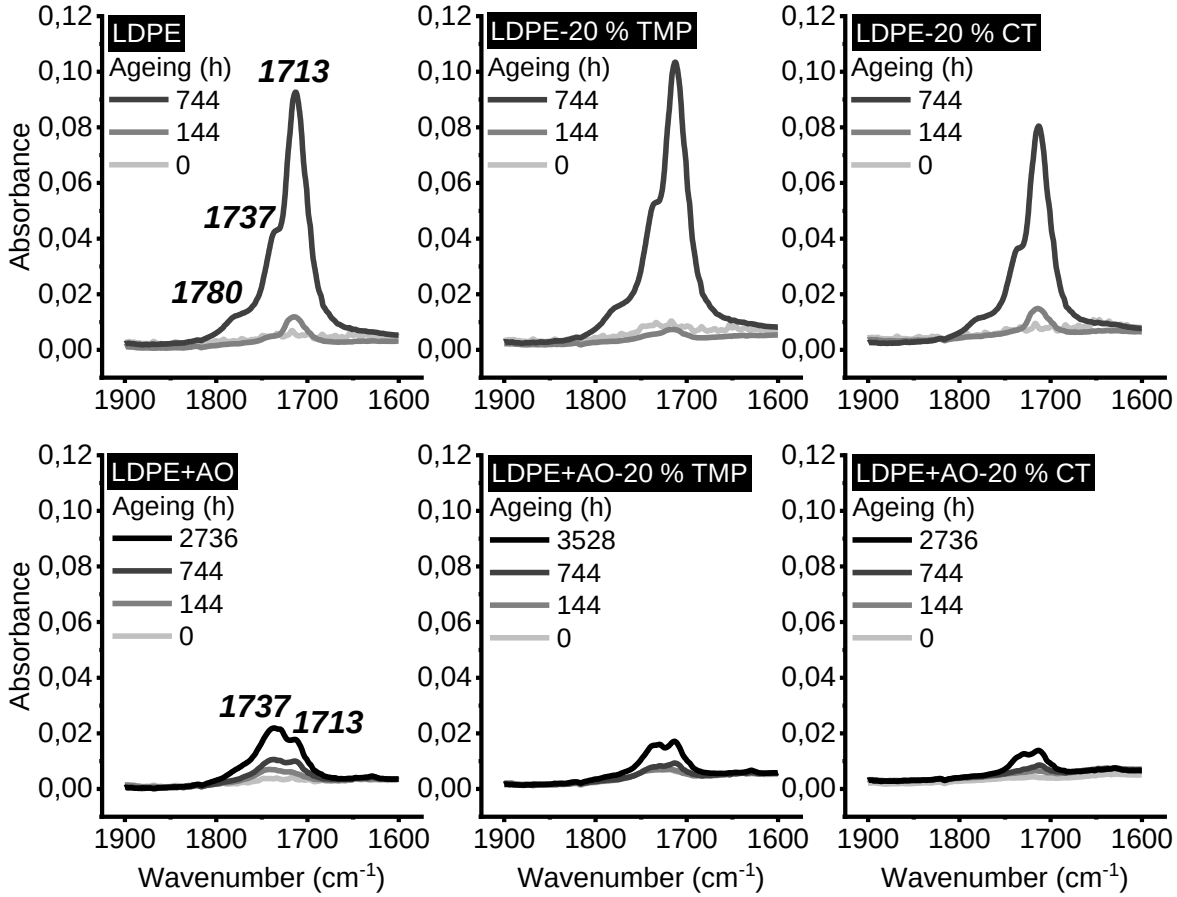

Figure 13: FTIR-ATR spectra between 1600 and 1900 cm^{-1}, showing the carbonyl bands

4.2.4 Rheological properties

Figure 14a shows the shear viscosity as a function of the shear rate between 1 and 1000 s^{-1} for the dispersions containing untreated or surface-grafted CNC at a concentration of 1.3 wt.%. All the suspensions exhibited a pronounced shear thinning behaviour and the same was noted at a concentration of 0.65 wt.%, although the viscosity was lower. In the low shear rate region in Figure 14a, the dispersions of MorphCNC and diHexylCNC displayed viscosity up to ten times greater than the dispersion containing the unmodified CNC, but the dispersion containing diAllylCNC exhibited the highest viscosity. The curves for the different dispersions approached each other as the shear rate increased. Similarly, as shown in Figure 14b, surface grafting onto the CNC markedly increased the dynamic-mechanical moduli *G'* and *G"* compared with the values obtained for the dispersion with the unmodified CNC. These findings were substantiated by the decrease in the percolation threshold or gel point for the modified samples. The dispersions containing the unmodified CNC started to gel at approximately 2.5 wt.% CNC, whereas the dispersions with the surface-grafted material showed a gel-like behaviour already at 0.2 - 0.4 wt.%. The percolation threshold was determined as the concentration at which the storage and loss moduli overlapped over a significant region of the applied strain amplitude, as exemplified in Figure 14b for the dispersion containing unmodified CNC.

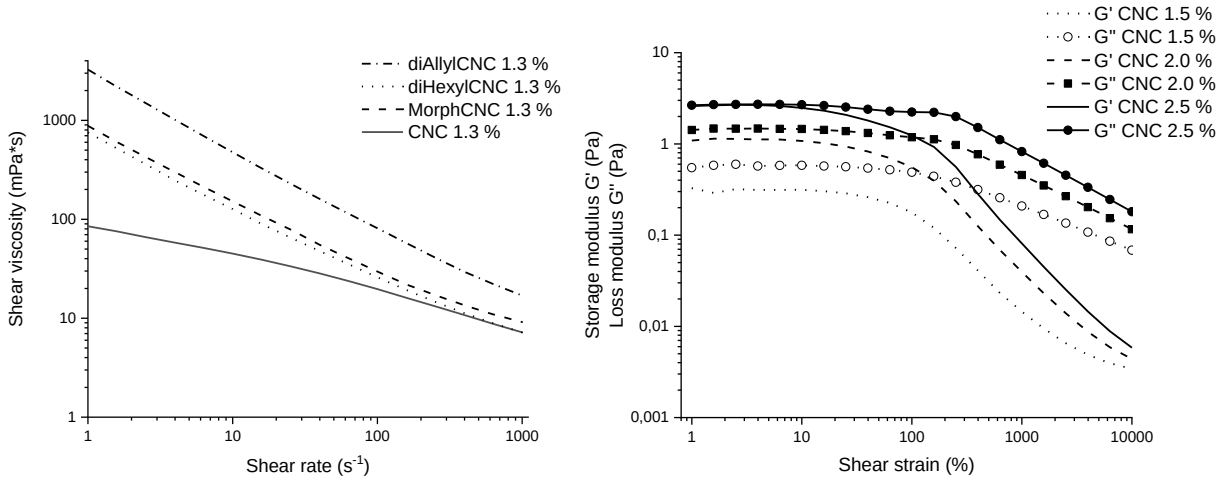

a) b)

Figure 14: a) The shear viscosity of the CNC-dispersions at a concentration of 1.3 wt.% as a function of the shear rate and b) the dynamic mechanical moduli at a frequency of 1 Hz and 25 °C as functions of the applied shear strain amplitude for aqueous dispersion containing different concentrations of untreated CNC. At a concentration of 2.5 wt.% CNC, the storage and loss moduli coincide over a substantial shear-strain region

These results show that surface treatment changes the interactions between the nanocrystals in the aqueous dispersions. The treated particles formed network structures already at lower concentrations, probably due to stronger molecular interactions leading to

an increase in viscosity and an increase in the dynamic moduli. The grafted azetidinium salts are primarily lipophilic, compared to the otherwise hydrophilic nature of CNC. In the aqueous dispersions, the substituents are prone to interact with each other more than with the surrounding water, forming a network to reduce their contact with water.

The different grafted azetidinium salts affect the rheological properties to different degrees, and the magnitude of the effect probably depends on the strength of the intermolecular bonding of the substituents. The main molecular interaction between alkyl groups is due to van der Waals forces, and this applies to the Morph and diHexyl substituents. The length of the substituents may also affect the shear viscosity, so that the longer diHexyl structure may give a more flexible network than the stiffer and smaller Morph structure. The diAllyl showed a significantly higher shear viscosity, possibly associated with the stronger molecular interaction of π-π-bonds of the allyl functionality acting between the substituents.

The CNC composites with EAA7 or LDPE as matrix material, produced by wet mixing in TSE, were evaluated with regard to their rheological properties. Figure 15 shows the shear viscosity of the composite melts at 170 °C as a function of the shear rate (after application of the Bagley and Rabinowitch corrections). A shear thinning behaviour was observed in all cases, and the shear viscosities were in general of the same magnitude. In more detail, the EAA7-based melts exhibited a somewhat higher viscosity than those based on LDPE. In the case of EAA7, the addition of CNC resulted in an increase in viscosity at a given shear rate compared to that of the unfilled polymer. In this case, the surface treatment of the CNC appeared to reduce the viscosity slightly relative to that of the melt containing untreated CNC. The viscosities of the LDPE-based melts were similar, but the highest viscosity was noted with the melt containing the surface-treated nanocellulose, but the differences were not as great as those observed with the aqueous CNC dispersions.

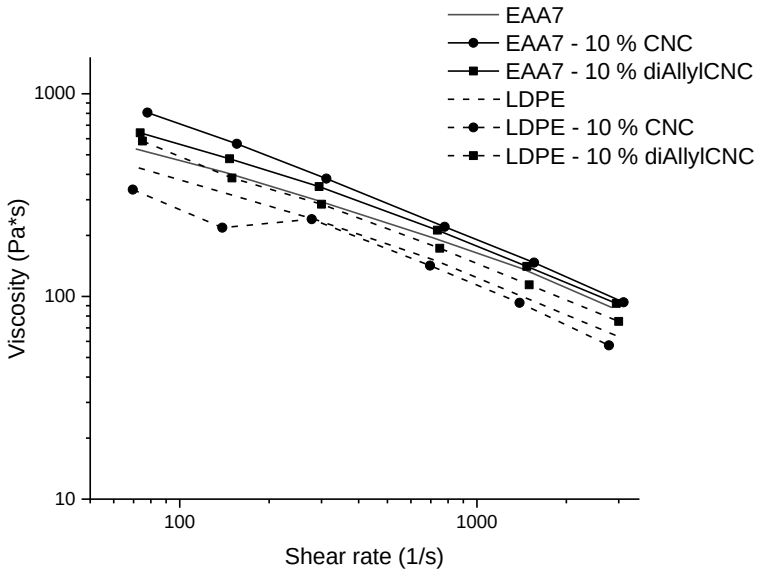

Figure 15: The shear viscosity of the CNC-composites as a function of the shear rate

The injection moulded CNC composites were subjected to oscillatory shear forces in strain sweeps and frequency sweeps and the results are summarized in Figure 16. All the samples, with the exception of the EAA7-10 % CNC and EAA7-10 % diAllylCNC materials, exhibited a *G'* plateau over the entire shear strain range in the oscillatory strain sweep (Figure 16a). The EAA7-based materials containing the unmodified CNC had a higher *G'* than those containing the surface-treated CNC. This was similar to the pattern noted for the tensile modulus, as described in section 4.3. In contrast, both the unmodified and modified CNC-reinforced samples exhibited a *G'* that increased with increasing strain amplitude up to a certain critical shear strain after which it decreased. This "overshoot" of *G'*, has also been observed in polymers and complex systems with a structural network that resists deformation up to a certain critical strain[80,81]. In our case, the overshoot was observed only for the *G'* value; as the loss modulus *G''* remained constant. The LDPE-based composites exhibited no such behaviour, however, and the CNC-reinforced samples actually exhibited lower *G'* values than the matrix polymer, the samples containing the unmodified CNC having the lowest values.

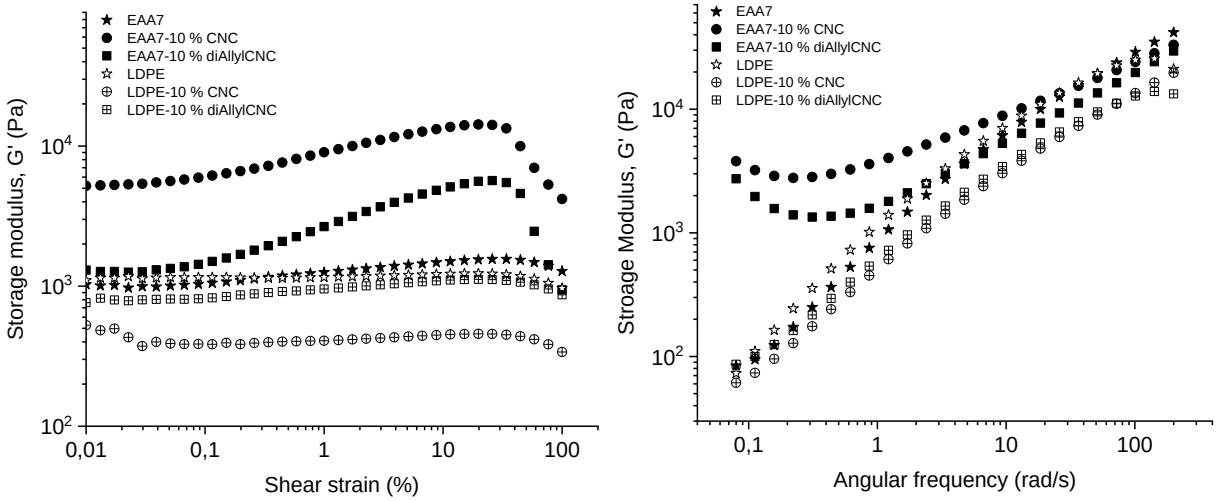

Figure 16: The storage moduli (G') as a function of (a) shear strain amplitude and (b) angular frequency for EAA (filled symbols) and LDPE (unfilled symbols) composites reinforced with unmodified and modified CNC

In the frequency sweep, Figure 16b, the EAA7 based samples containing CNC clearly differed. The samples exhibited a pronounced plateau at lower frequencies and the EAA7 containing unmodified CNC showed the highest *G'* values. The plateau at lower frequencies is observed in systems in which a structural network is formed[50,82,83]. This plateau was not observed in the case of the LDPE samples reinforced with CNC which behaved in a manner similar to that of the matrix material. They also displayed lower *G'* values than the unfilled LDPE. This behaviour was also seen in the mechanical properties. There was little variation

in the strength of the LDPE composites reinforced with CNC, which could be related to the absence of a percolated network in the material, cf section 4.3.1.

4.2.5 Characterization of the surface-grafting

FTIR, ζ–potential measurements and conductometric titration in addition to the thermal stability measurements (TGA) described in section 4.2.1, were used for the characterisation of the surface-grafting, the results of which are reported in detail in Papers I, II and V.

The FTIR spectra showed a peak shift corresponding to a change in the sulphate ester bond absorption, indicating substitution on the sulphate ester supporting the hypothesis that the grafting had been achieved. The higher ζ-potential values noted for the modified nanocrystals, indicated that the modified CNC had fewer sulphuric groups on the surface and thus that grafting had occurred. The sulphate half ester content on the CNC surface was determined by conductometric titration, and the lower values of surface charge on the surface-grafted samples showed that the reagents had reacted with the negatively charged sulphate groups.

It was therefore concluded that the surface grafting on the sulphate half esters on the CNC surface was successful.

4.3 MECHANICAL PROPERTIES

4.3.1 Tensile properties

The incorporation of the wood-based reinforcement into the polymer matrix had a significant effect on the tensile properties of all types of reinforcements and matrices. The different reinforcement and matrix materials were however processed by different techniques and this means that the results may not be comparable unless these differences are taken into account. It is nevertheless interesting to study the differences when trying to tailor the mechanical properties of the composites. The Young's modulus, yield stress (when applicable), ultimate tensile strength and elongation at break for all the composites used in this project are summarized in Table 5.

In the first small- scale production of CNC composites using dispersion mixing, air drying and compression moulding, the reinforcement of EAA15 with 10 wt.% CNC had a strong positive effect on the Young's modulus. As shown in Figure 17, the modulus increased from ca 300 MPa to more than 900 MPa with the untreated CNC, closely followed by the EAA15-10 % diAllylCNC. At the lower concentrations of 0.1 and 1 wt.%, the effect was however small.

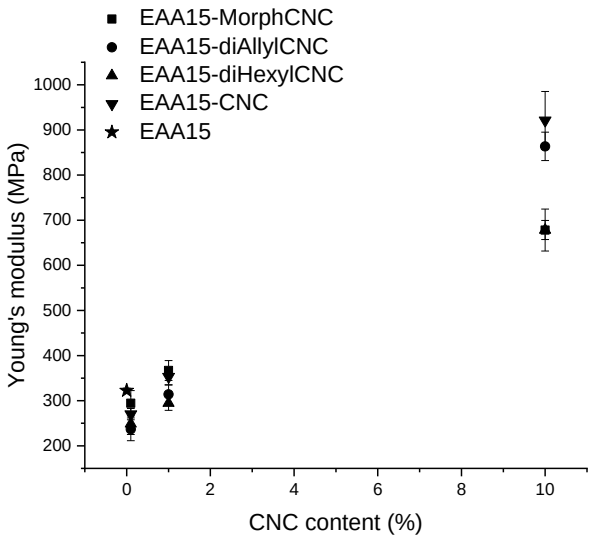

Figure 17: a) Young's modulus and b) yield stress of the compression moulded EAA15 composites, reinforced with three surface-modified or unmodified CNC, as a function of the CNC-content

With a low concentration of CNC, the material appeared to be more ductile than the EAA15 matrix itself, as shown in Table 5. The elongation at break increased with a low concentration of CNC, which has been seen before when a filler is added to a matrix[84]. The increased ductility may be interpreted as being due to interactions between the surface-modified nanocrystals and also between the nanocrystals and the matrix polymer, as discussed in detail in Paper II.

With water-assisted extrusion and injection moulding of 10 wt.% CNC composites with EAA7 pellets or LDPE, the increase in mechanical properties was smaller. The change of mixing and processing techniques used, together with the slight change of materials, had a major effect on the final properties of the composite. The Young's modulus increased by 50-100 % when the EAA7 or LDPE matrix was reinforced with 10 wt.% unmodified or diallyl-modified CNC. The difference in processing may have affected the dispersion and interaction between the matrix and reinforcing element but the mechanical properties may also have been significantly influenced by the shaping. The injection moulding process involves a strong orientational flow leading to an oriented morphology in the material. The compression-moulded EAA15 displayed a stiffness almost 300 % higher than that of the injection-moulded EAA7. Reference samples were produced using aqueous dispersed EAA7 or EAA15, reinforced with CNC from CelluForce and surface modified using both hydroxyazetidinium salts and a carbonate reagent. All these combinations were dispersion mixed, air dried and compression moulded as reported in Paper II. The strong increase in the Young's modulus seen in the compression-moulded samples in Paper II was also found with the CelluForce-CNC with both EAA15 and EAA7 as matrix material. The difference in CNC grade did not seem to influence the stiffness of the material significantly, but the ductility of the material was significantly greater for the diallyl-modified EAA samples, giving an elongation at break similar to that of the neat matrix material. The EAA15-10 % diAllylCNC with CelluForce CNC exhibited a greater elongation to break than the same

material containing CNC produced from MCC which instead exhibited a large increase in yield stress.

The yield stress was increased slightly when 10 wt.% surface-modified CNC was added to the compression-moulded composites, but the effect was more pronounced with the injection-moulded EAA7-10 % CNC and EAA7-10 % diAllylCNC, where the increase was 40-120 %. The elongation at break was enhanced by the diallyl treatment of CNC in the injection-moulded EAA7 matrix compared with the EAA7 composite with unmodified CNC.

In the case of the compression-moulded samples with 10 wt.% CNC in Paper II, the Young's modulus of the CNC was estimated to be between 55 and 60 GPa using the Cox-Krenchel equation [32,85,86], described in Paper II. This estimation was made using the values of tensile moduli given in Table 5, assuming perfect adhesion between the matrix and the CNC. 55-60 GPa is a rather high value, approaching the value for glass fibres (70 GPa) and surpasses or is close to previous values reported for the effective modulus of cellulose nanofibrils (CNF), e. g. 29-36 GPa [87], 33-62 GPa [88] and 25-42 GPa [89].

The tensile modulus of both EAA7 and LDPE was also clearly improved by the addition of TMP or CT/CF as reinforcing agent. An addition of 20 wt.% resulted in a higher stiffening effect than an addition of 5 wt.%. The addition of 20 wt.% CF into EAA7 (injection moulded) increased the elastic modulus by a factor of approximately 3, whereas the addition of 20 wt.% CT into a LDPE matrix (SSE) approximately doubled the modulus. The addition of antioxidant slightly increased the elastic modulus of the TMP-reinforced or CT-reinforced samples but did not change the properties of the neat LDPE matrix, possibly due to a decrease in degradation of the reinforcement during processing which did not occur with the neat LDPE.

The effect of the ageing was markedly affected by the presence of antioxidant as can be seen in Figure 18. The elongation at break decreased with increasing ageing time in the case of samples without antioxidant, whereas it did not change significantly in the case of samples with antioxidant. Ageing had a significant effect on the tensile strength of any of the samples.

Table 5: Mechanical properties of the composite materials, with different reinforcements, matrices and processing techniques. Standard deviations in parentheses

Comment	Material	Young's modulus (MPa)	Yield stress (MPa)	Ultimate tensile strength (MPa)	Elongation at break (%)
CNC from MCC, AzOH-modified, dispersion-mixed, air dried, compression-moulded (Paper II)	EAA15	322 (5)	15.1 (0.6)	25.8 (1.2)	255 (6)
	EAA15-0.1 % CNC	270 (13)	13.5 (0.3)	24.5 (0.7)	278 (6)
	EAA15-0.1 % MorphCNC	294 (28)	14.1 (0.5)	24.3 (0.8)	284 (11)
	EAA15-0.1 % diAllylCNC	237 (25)	12.1 (1.0)	21.2 (1.3)	276 (11)
	EAA15-0.1 % diHexylCNC	249 (24)	12.8 (0.6)	23.5 (1.4)	288 (15)
	EAA15-1 % CNC	353 (18)	15.3 (0.5)	25.3 (1.7)	246 (7)
	EAA15-1 % MorphCNC	367 (22)	15.2 (0.6)	23.4 (1.3)	252 (10)
	EAA15-1 % diAllylCNC	314 (21)	14.1 (0.6)	22.9 (1.0)	261 (10)
	EAA15-1 % diHexylCNC	295 (16)	14.1 (0.4)	23.7 (1.2)	267 (10)
	EAA15-10 % CNC	921 (64)	-	21.9 (0.9)	6 (1)
	EAA15-10 % MorphCNC	678 (46)	15.1 (0.4)	14.2 (2.3)	11 (10)
	EAA15-10 % diAllylCNC	864 (32)	21.1 (0.7)	19.7 (0.8)	31 (22)
	EAA15-10 % diHexylCNC	678 (21)	17.9 (0.4)	16.5 (1.0)	28 (15)
CelluForce CNC, AzOH-modified produced as in Paper II (reference)	EAA7-10 % CNC	860 (21)	-	18 (0.4)	88 (20)
	EAA7-10 % diAllylCNC	783 (27)	-	16 (0.3)	58 (8)
	EAA15-10 % CNC	948 (35)	-	23 (0.2)	8 (0.7)
	EAA15-10 % diAllylCNC	697 (17)	16 (0.2)	22 (1)	206 (18)
	EAA15-10 % diAllylCNC (Carbonate modified)	544 (14)	14 (0.2)	17 (2)	115 (43)
CelluForce CNC, Carbonate modified, wet-mixed, TSE, injection-moulded (Paper V)	EAA7	109 (2)	5.7 (0.1)	16.8 (0.6)	90.6 (2.6)
	EAA7-10 % CNC	197 (14)	12.9 (0.3)	17.5 (0.3)	36.7 (3.6)
	EAA7-10 % diAllylCNC	166 (4)	8 (0.2)	16 (0.5)	59 (3.2)
	LDPE	150 (7)	7 (0.1)	13 (0.3)	62 (3.6)
	LDPE-10 % CNC	210 (2)	8.5 (0.3)	12.1 (0.3)	39.4 (1)
	LDPE-10 % diAllylCNC	209 (6)	9 (0.2)	12.6 (0.1)	38 (2.1)
TMP or CT, TSE mixed, SSE (Paper IV)	LDPE	269 (14)	-	10.6 (3.1)	346 (81)
	LDPE-5 % TMP	298 (8)	-	9.8 (0.3)	27 (4.7)
	LDPE-20 % TMP	533 (38)	-	13.5 (0.4)	7 (0.4)
	LDPE-5 % CT	308 (19)	-	10.0 (0.4)	33 (7.3)
	LDPE-20 % CT	480 (21)	-	15.5 (0.5)	9 (1.0)
	LDPE+AO	272 (25)	-	11.6 (1.8)	263 (158)
	LDPE+AO-5 % TMP	339 (35)	-	9 (0.4)	29 (4.9)
	LDPE+AO-20 % TMP	644 (10)	-	12 (0.1)	5 (0.7)
	LDPE+AO-5 % CT	307 (20)	-	10 (0.2)	32 (4.8)
	LDPE+AO-20 % CT	553 (20)	-	12 (0.6)	7 (0.9)
CF, TSE mixed, Injection-moulded (Paper III)	EAA7 170 °C	112 (5)	-	16 (0.5)	92 (8)
	EAA7 200 °C	114 (5)	-	18 (0.8)	124 (8)
	EAA7 230 °C	114 (4)	-	22 (0.1)	174 (15)
	EAA7-20 % CF 170 °C	354 (13)	-	16 (0.3)	29 (1)
	EAA7-20 % CF 200 °C	353 (17)	-	17 (0.1)	34 (1)
	EAA7-20 % CF 230 °C	354 (15)	-	16 (0.2)	42 (3)

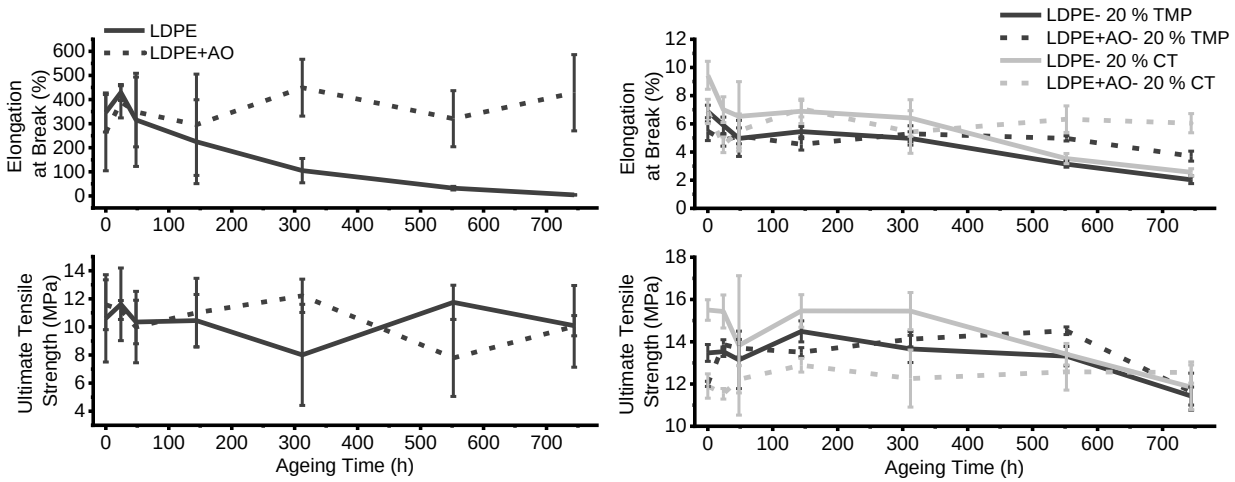

a) b)

Figure 18: The effect of ageing time on the elongation at break and ultimate tensile strength of a) neat LDPE with and without AO and b) LDPE composites reinforced with 20 wt.% TMP or CT with and without AO

The trials with different processing temperatures and browning of the 20 wt.% CF-reinforced samples did not have any significant effect on the mechanical properties. The stiffness and strength of the composite materials were more or less unchanged, whereas the elongation at break increased somewhat when a higher processing temperature was used. This was even more evident for the pure EAA7 matrix which also showed an increase in ultimate tensile strength when the process temperature was increased, as shown in Figure 19. Further studies based on shrinkage measurements and polarized light microscopy revealed differences in orientation between samples moulded at different melt temperatures. It appears that interactions associated with the acrylic acid comonomer can create a network structure in the samples. This is further discussed in Paper III.

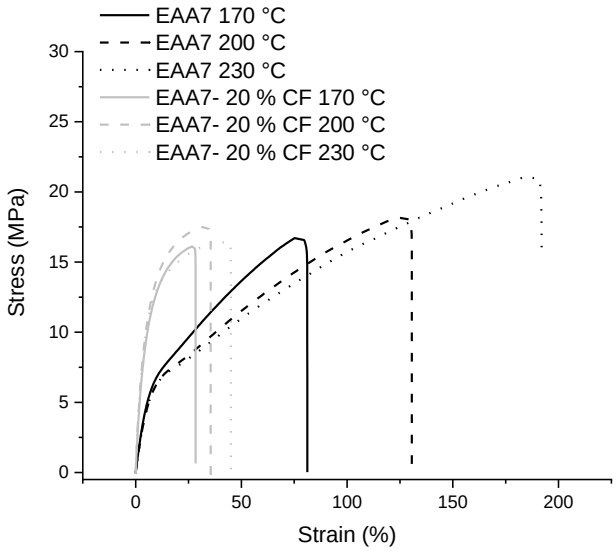

Figure 19: Stress-strain curves for the EAA7-20 % CF composites and the neat EAA7 matrix, injection-moulded at different process temperatures

4.3.2 Dynamic-mechanical analysis

Figure 20 shows the mechanical loss factor (tan δ) as a function of the strain amplitude of the applied sinusoidal deformation for (a) the dispersion-mixed and compression-moulded composites with 10 wt.% CNC and (b) the water-assisted extruded and injection-moulded composites with 10 wt.% CNC, in comparison with the neat matrices. The difference in the slope of the loss factor (amplitude) curve between the composite and the matrix can provide information about the properties of the interphase region between the matrix and the reinforcement [84,90].

The surface grafting clearly affected the mechanical loss factor of the compression moulded specimen (Figure 4), as can be seen in Figure 20a, where the surface modification with diHexyl and Morph gave a somewhat higher loss factor than the composite with unmodified CNC which was less sensitive to an increase in strain amplitude. The surface treatment may lead to a flexible interphase region close to the CNC. The composite containing 10 wt.% diAllylCNC had the lowest tan δ value with a weak dependence on the strain amplitude, indicating a rather strong interphase region.

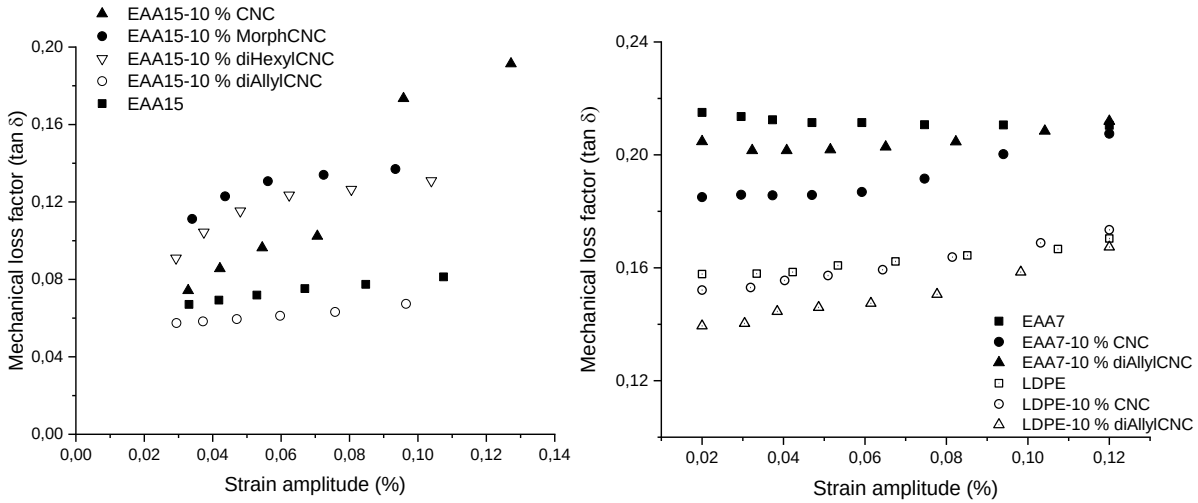

a) b)

Figure 20: The mechanical loss factor as a function of the applied strain amplitude for a) compression-moulded EAA15 composites containing 10 wt.% CNC , either surface modified or unmodified and the neat EAA15 matrix and b) injection-moulded EAA7 and LDPE composites containing 10 wt.% CNC, either surface modified or unmodified and the neat EAA7 matrix

These findings were confirmed by the mechanical loss factor of the composites produced by water-assisted extrusion and injection moulding in Paper V, as shown in Figure 20b. The magnitude of the loss factor was not significantly different for the samples having the same matrix material. The loss factor was only weakly dependent on the applied deformation at high strain amplitudes in the case of the EAA7 reinforced with diAllylCNC compared with the unmodified CNC, indicating a more stable interphase region. This was to some extent supported by the greater extensibility of the composite, cf Table 5. With LDPE as the

matrix, the loss factor of the composites with CNC increased more with increasing imposed deformation than that of the unfilled polymer, and there were no significant differences between the modified and unmodified CNC.

Accelerated ageing for 744 h did not significantly affect the mechanical loss factor of LDPE reinforced with 20 wt.% TMP or CT, whether with or without added AO, as can be seen in Figure 21. There was thus no indication of any significant weakening of the interphase region between the fibre and matrix in this case.

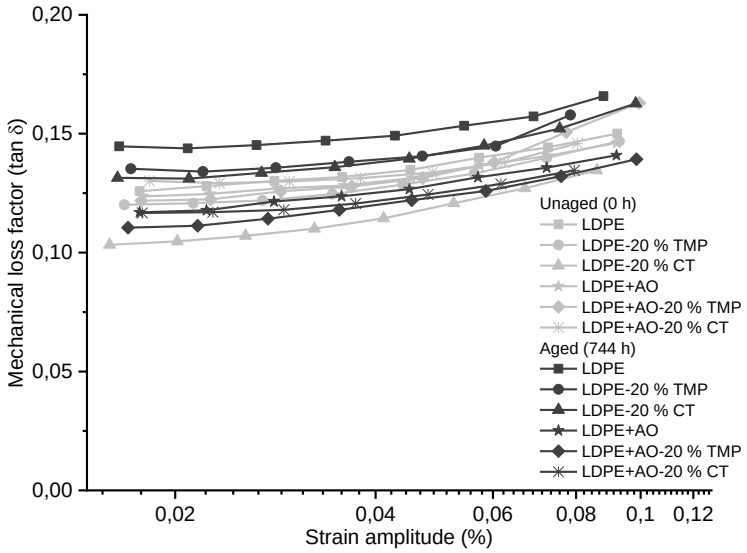

Figure 21: The mechanical loss factor as a function of the applied strain amplitude for LDPE composites reinforced with 20 wt.% TMP or CT, with and without AO, before and after 744 h of accelerated ageing

5 CONCLUSIONS

The addition of 5-20 wt.% cellulose-based reinforcement, regardless of the size or type, improved the mechanical properties compared to those of the neat polymer matrices, with an increase of 50-300 % in the tensile Young's modulus. Theoretically, cellulose nanocrystals should have a stronger reinforcing effect than the larger fibres due to their greater specific stiffness and high aspect ratio, but the mechanical properties are also greatly affected by the processing method, where the dispersion-mixed, air-dried and compression-moulded CNC composites exhibited a greater increase in the mechanical properties than the injection-moulded CNC samples mixed by water-assisted extrusion and compounding. When a continuous processing technique such as extrusion was used, the increase in tensile modulus of the CNC composite was similar to that of the composites reinforced with larger fibres from cellulose tissue or thermomechanical pulp. This may be due to a tendency to form large aggregates or not to be homogeneously dispersed.

Continuous large-scale conventional processing techniques have been used to produce CNC composites using water-assisted mixing to successfully produce homogeneous material in a steady state. However, dispersion mixing still seems to be the best option to keep the nanoparticles apart, avoid aggregation and obtain favourable mechanical properties. Without any obvious solution for performing dispersion mixing on a large scale, it seems important to continue to adjust the process parameters to maintain nano-sized particles in the future of continuous processing. The process parameters have a great effect on the resulting material, and minor changes in temperature, residence time, pressure, technique, feeding rate etc. would have a significant impact.

The choice of surface modification seems to affect the adhesion and network formation within the composite, by an interaction both between the reinforcement and the polymer matrix and between the reinforcing elements, resulting in ductile and flexible materials especially with low reinforcement content. The surface-modified CNC clearly promoted an internal network in aqueous dispersion, lowering the percolation threshold significantly. It was also shown that it is possible to increase or maintain thermal stability of CNC by surface modification, depending on the surface chemistry of the CNC used.

Colour changes caused by exposure to elevated temperatures were visible early in the degradation process but, even with significant discoloration and browning, the mechanical properties of the material were not significantly affected.

The addition of wood-based reinforcement did not reduce the resistance towards thermal degradation during ageing. In fact, the addition of a lignin-containing reinforcement significantly increased the resistance towards thermo-oxidative ageing, especially in combination with an added antioxidant.

6 FUTURE WORK

Further studies might explore the use of other matrix material with cellulose reinforcement. This would include engineering polymers with better mechanical properties such as polyamides, for use in more long-term load-bearing applications. Bio-based or biodegradable matrix materials would also be of interest, to produce compostable composites for short-term-use products.

The surface treatment and modification of the CNC as well as the larger cellulose-based fibres could be further advanced, e.g. by exploring the possibilities of tailoring the properties of a given system of reinforcement and polymer matrix to improve adhesion, dispersion, thermal and mechanical properties.

The processing and resulting properties should be further studied to optimize the production method, to ease the upscaling and make it more feasible for industrial use by understanding and predicting flow behaviour and the optimum process parameters. The feasibility of using moisture or not in the mixing and compounding step should be further evaluated, to see whether moisture can increase the dispersion and adhesion significantly or merely create difficulties during processing with excess water in the system. Other screw configurations should be studied to possibly increase the dispersion or the adhesion between reinforcement and fibre, i.e. to maximise the reinforcing effect. The second extrusion step is expected to improve the dispersion and mixing, but further studies are required to assess whether there is a risk that the prolonged exposure time to elevated temperature and shear forces may initiate significant thermal degradation.

The durability of the material should be further studied to be able to predict the long-term behaviour of the materials before they are confidently implemented by industry. This includes an analysis of the ageing behaviour and its effect on the thermal and mechanical properties as well as on the appearance and surface characteristics.

If a non-biodegradable polymer matrix is still used, it will probably be very important to consider the handling after the first lifecycle of the material, i. e. to look in more detail into issues such as reusability (hence durability), recycling or incineration. The recycling of thermoplastic composites in general could be performed mechanically, thermally or chemically, but there are as yet no commercial operations for the recycling of composite materials in an economic way[91]. Reinforcements commonly used in packaging plastics may cause problems during the separation of different polymer types before mechanical recycling and they may cause contamination if they cannot be separated with the techniques used today. The discussion regarding the after-life of the first lifecycle needs to be further expanded to find strategies and solutions to use these materials in as sustainable a way as possible.

7 ACKNOWLEDGEMENT

I wish to express my deepest gratitude to both my supervisors, Mikael Rigdahl and Antal Boldizar, for all the interesting discussions and all the knowledge you have shared so generously, and not least for your superior "coaching", providing a great working environment where I have been challenged but have always felt your support, making it possible for me to explore and develop both confident and new knowledge. It has been a privilege working with you.

The Swedish Research Council Formas and the Swedish Foundation for Strategic Research is gratefully acknowledged for the financial support during the project. Dr J. A. Bristow is gratefully acknowledged for the linguistic revision of the article manuscripts and the thesis.

I would like to thank my co-authors and much appreciated colleagues Karin Sahlin-Sjövold and Gunnar Westman from the Department of Chemistry and Chemical Engineering for great collaboration, many hours together in the laboratory and fruitful discussions. I have learnt so much from you. I would also like to thank Alberto Vega, Nazdaneh Yarahmadi and Johan Berglund from RISE for the use of equipment, and most of all for the great collaborations and discussions, writing articles together.

I would like to thank my colleagues and in some cases co-authors from the polymer group; Ezgi Ceren Boz Noyan, Angelica Avella, Sylwia Wojno, Bashar Haseeb, Kristina Karlsson, Johannes Thunberg, Tobias Moberg, Karolina Gaska, Georgia Manika, Roland Kadar, Fabiola Vilaseca Morera and Giada Lo Re for many great discussions, hours in the laboratory, coffee breaks, conference trips and for all I have learnt from you. Special thanks to Abhijit Venkatesh for saving me so many times and always having my back. It has been great teamwork.

Special thanks to Håkan Millqvist and Roger Sagdahl for all the help in the laboratory and with technical issues, always finding some way to solve things. Marcus Folino is acknowledged for taking nice photographs of my samples.

I would like to thank all my colleagues at the Department of Industrial and Materials Science, both present and former, for all the great times and memories created during these years, from ski-trips and floorball games to conferences or just everyday coffee breaks.

Last but not least, I would like to thank my friends and family, my parents for being unconditionally interested and supportive, brothers and friends for giving some perspective to my work by being curious, by asking questions outside the box and by getting so easily impressed by my work, and thank you, Daniel, for your love and support through all dimensions of life.

8 REFERENCES

1. Berggren K, Klason C and, Kubat J. Spritzgiessen holzmehlhaltiger Thermoplaste. *Kunststoffe*. 1975;65(2):69-74.

2. Klason C, Kubát J, Strömvall H-E. The Efficiency of Cellulosic Fillers in Common Thermoplastics. Part 1. Filling without Processing Aids or Coupling Agents. *Int J Polym Mater Polym Biomater*. 1984;10(3):159-187. doi:10.1080/00914038408080268

3. Domininghaus H. *Plastics for Engineers*. Hanser Gardner Publications; 1999.

4. Miao C, Hamad WY. Cellulose reinforced polymer composites and nanocomposites: A critical review. *Cellulose*. 2013;20(5):2221-2262. doi:10.1007/s10570-013-0007-3

5. Kokta B V., Chen R, Daneault C, Valade JL. Use of wood fibers in thermoplastic composites. *Polym Compos*. 1983;4(4):229-232. doi:10.1002/pc.750040407

6. Bledzki AK, Faruk O, Sperber VE. Cars from Bio-Fibres. *Macromol Mater Eng*. 2006;291(5):449-457. doi:10.1002/mame.200600113

7. Bledzki AK, Gassan J. Composites reinforced with cellulose based fibres. *Prog Polym Sci*. 1999;24(2):221-274. doi:10.1016/S0079-6700(98)00018-5

8. Jawaid M, Abdul Khalil HPS. Cellulosic/synthetic fibre reinforced polymer hybrid composites: A review. *Carbohydr Polym*. 2011;86(1):1-18. doi:10.1016/j.carbpol.2011.04.043

9. Sharma A, Thakur M, Bhattacharya M, Mandal T, Goswami S. Commercial application of cellulose nano-composites – A review. *Biotechnol Reports*. 2019;21:e00316. doi:10.1016/j.btre.2019.e00316

10. Gholampour A, Ozbakkaloglu T. A review of natural fiber composites: properties, modification and processing techniques, characterization, applications. *J Mater Sci*. 2020;55(3):829-892. doi:10.1007/s10853-019-03990-y

11. Kalia S, Dufresne A, Cherian BM, et al. Cellulose-based bio- and nanocomposites: A review. *Int J Polym Sci*. 2011;2011. doi:10.1155/2011/837875

12. Bledzki AK, Letman M, Viksne A, Rence L. A comparison of compounding processes and wood type for wood fibre - PP composites. *Compos Part A Appl Sci Manuf*. 2005;36(6):789-797. doi:10.1016/j.compositesa.2004.10.029

13. Dalväg H, Klason C, Strömvall H-E. The Efficiency of Cellulosic Fillers in Common Thermoplastics. Part II. Filling with Processing Aids and Coupling Agents. *Int J Polym Mater*. 1985;11(1):9-38. doi:10.1080/00914038508078651

14. Kaplan D. *Biopolymers from Renewable Resources*. Springer; 1998.

15. Campilho RDSG. *Natural Fiber Composites*. 1st ed. CRC Press; 2015.

16. *Forest Statistics 2020*.; 2020. Accessed September 10, 2020. www.slu.se/riksskogstaxeringen

17. Henriksson G, Brännvall E, Lennholm H. *The Ljungberg Textbook Wood Chemistry*. Forest Production and Chemical Engineering, Department of Chemical and Biological

Engineering, Chalmers University of Technology; 2008.

18. Fellers C, Norman B. *Pappersteknik*. Avdelningen för pappersteknik, Kungliga Tekniska Högskolan; 1996.

19. Rowell RM. *Handbook of Wood Chemistry and Wood Composites* . 2nd ed. CRC Press; 2013. doi:10.1201/b12487

20. Habibi Y, Lucia LA, Rojas OJ. Cellulose nanocrystals: Chemistry, self-assembly, and applications. *Chem Rev*. 2010;110(6):3479-3500. doi:10.1021/cr900339w

21. Ardanuy M, Claramunt J, Toledo Filho RD. Cellulosic fiber reinforced cement-based composites: A review of recent research. *Constr Build Mater*. 2015;79:115-128. doi:10.1016/j.conbuildmat.2015.01.035

22. Bandyopadhyay-Ghosh S, Ghosh SB, Sain M. The use of biobased nanofibres in composites. In: *Biofiber Reinforcements in Composite Materials*. Elsevier Inc.; 2015:571-647. doi:10.1533/9781782421276.5.571

23. Meng Z, Qi K, Guo Y, Wang Y, Liu Y. Effects of thickening agents on the formation and properties of edible oleogels based on hydroxypropyl methyl cellulose. *Food Chem*. 2018;246:137-149. doi:10.1016/j.foodchem.2017.10.154

24. Pervaiz M, Panthapulakkal S, KC B, Sain M, Tjong J. Emerging Trends in Automotive Lightweighting through Novel Composite Materials. *Mater Sci Appl*. 2016;07(01):26-38. doi:10.4236/msa.2016.71004

25. Klason C, Kubat J, Stromvall H-E. The efficiency of cellulosic fillers in common thermoplastics. Part 1. Filling without processing aids or coupling agents. *Int J Polym Mater*. 1984;10(May 2016):159-187. doi:10.1080/00914038508078651

26. Emsley AM. The kinetics and mechanisms of degradation of cellulosic insulation in power transformers. *Polym Degrad Stab*. 1994;44(3):343-349. doi:10.1016/0141-3910(94)90093-0

27. Sapieha S, Pupo JF, Schreiber HP. Thermal degradation of cellulose-containing composites during processing. *J Appl Polym Sci*. 1989;37(1):233-240. doi:10.1002/app.1989.070370118

28. Clarkson CM, El Awad Azrak SM, Forti ES, Schueneman GT, Moon RJ, Youngblood JP. Recent Developments in Cellulose Nanomaterial Composites. *Adv Mater*. Published online July 21, 2020:2000718. doi:10.1002/adma.202000718

29. Beck-Candanedo S, Roman M, Gray DG. Effect of reaction conditions on the properties and behavior of wood cellulose nanocrystal suspensions. *Biomacromolecules*. 2005;6(2):1048-1054. doi:10.1021/bm049300p

30. Rånby BG. Fibrous macromolecular systems. Cellulose and muscle. The colloidal properties of cellulose micelles. *Discuss Faraday Soc*. 1951;11(0):158-164. doi:10.1039/DF9511100158

31. Moberg T, Sahlin K, Yao K, et al. Rheological properties of nanocellulose suspensions: effects of fibril/particle dimensions and surface characteristics. *Cellulose*. 2017;24(6):2499-2510. doi:10.1007/s10570-017-1283-0

32. Lee KY, Aitomäki Y, Berglund LA, Oksman K, Bismarck A. On the use of nanocellulose as reinforcement in polymer matrix composites. *Compos Sci Technol*. 2014;105:15-27. doi:10.1016/j.compscitech.2014.08.032

33. Klemm D, Kramer F, Moritz S, et al. Nanocelluloses: A new family of nature-based materials. *Angew Chemie - Int Ed*. 2011;50(24):5438-5466. doi:10.1002/anie.201001273

34. Wang N, Ding E, Cheng R. Thermal degradation behaviors of spherical cellulose nanocrystals with sulfate groups. *Polymer (Guildf)*. 2007;48(12):3486-3493. doi:10.1016/j.polymer.2007.03.062

35. Roman M, Winter WT. Effect of Sulfate Groups from Sulfuric Acid Hydrolysis on the Thermal Degradation Behavior of Bacterial Cellulose. Published online 2004. doi:10.1021/BM034519

36. Oksman K, Aitomäki Y, Mathew AP, et al. Review of the recent developments in cellulose nanocomposite processing. *Compos Part A Appl Sci Manuf*. 2016;83:2-18. doi:10.1016/j.compositesa.2015.10.041

37. Gan PG, Sam ST, Abdullah MF bin, Omar MF. Thermal properties of nanocellulose-reinforced composites: A review. *J Appl Polym Sci*. 2020;137(11):48544. doi:10.1002/app.48544

38. Börjesson M, Westman G. Crystalline Nanocellulose — Preparation, Modification, and Properties. In: *Cellulose - Fundamental Aspects and Current Trends*. InTech; 2015. doi:10.5772/61899

39. Mosca Conte A, Pulci O, Knapik A, et al. Role of cellulose oxidation in the yellowing of ancient paper. *Phys Rev Lett*. 2012;108(15). doi:10.1103/PhysRevLett.108.158301

40. Shafizadeh F, Bradbury AGW. Thermal degradation of cellulose in oxygen and nitrogen at high temperatures. *J Appl Polym Sci*. 1979;23:1431-1442. doi:10.1002/app.1979.070230513

41. Klyosov AA. Wood-Plastic Composites | Wiley. In: *Wood-Plastic Composites*. John Wiley & Sons; 2007:493-584.

42. Sapieha S, Pupo JF, Schreiber HP. Thermal degradation of cellulose-containing composites during processing. *J Appl Polym Sci*. 1989;37(1):233-240. doi:10.1002/app.1989.070370118

43. European Bioplastics. Accessed September 10, 2020. https://www.european-bioplastics.org/market/

44. Geyer R, Jambeck JR, Law KL. Production, use, and fate of all plastics ever made. *Sci Adv*. 2017;3(7):e1700782. doi:10.1126/sciadv.1700782

45. Sanschagrin B, Sean ST, Kokta BV. Mechanical Properties of Cellulose Fibers Reinforced Thermoplastics. *J Thermoplast Compos Mater*. 1988;1(2):184-195. doi:10.1177/089270578800100206

46. Azizi Samir MAS, Alloin F, Sanchez JY, Dufresne A. Cellulose nanocrystals reinforced poly(oxyethylene). *Polymer (Guildf)*. 2004;45(12):4149-4157. doi:10.1016/j.polymer.2004.03.094

47. Zheng T, Pilla S. Melt Processing of Cellulose Nanocrystal-Filled Composites: Toward Reinforcement and Foam Nucleation. Published online 2020. doi:10.1021/acs.iecr.0c00170

48. Karger-Kocsis J, Kmetty Á, Lendvai L, Drakopoulos S, Bárány T. Water-Assisted Production of Thermoplastic Nanocomposites: A Review. *Materials (Basel)*. 2014;8(1):72-95. doi:10.3390/ma8010072

49. Ariño R, Boldizar A. Processing and Mechanical Properties of Thermoplastic Composites Based on Cellulose Fibers and Ethylene - Acrylic Acids Copolymer. *Polym Eng Sci*. 2012;47:21-25. doi:10.1002/pen.23134

50. Abhijit V, Johannes T, Sahlin-Sjövold K, Mikael R, Boldizar A. Melt Processing of Ethylene-Acrylic Acid Copolymer Composites Reinforced with Nanocellulose. *Polym Eng Sci*. 2020;60(5):956-967. doi:10.1002/pen.25351

51. Azouz K Ben, Ramires EC, Van Den Fonteyne W, El Kissi N, Dufresne A. Simple method for the melt extrusion of a cellulose nanocrystal reinforced hydrophobic polymer. *ACS Macro Lett*. 2012;1(1):236-240. doi:10.1021/mz2001737

52. Le Baillif M, Oksman K. The Effect of Processing on Fiber Dispersion, Fiber Length, and Thermal Degradation of Bleached Sulfite Cellulose Fiber Polypropylene Composites. *J Thermoplast Compos Mater*. 2009;22(2):115-133.

53. Migneault S, Koubaa A, Erchiqui F, et al. Effect of fiber length on processing and properties of extruded wood-fiber/HDPE composites. *J Appl Polym Sci*. 2008;110(2):1085-1092. doi:10.1002/app.28720

54. Herrera N, Salaberria AM, Mathew AP, Oksman K. Plasticized polylactic acid nanocomposite films with cellulose and chitin nanocrystals prepared using extrusion and compression molding with two cooling rates: Effects on mechanical, thermal and optical properties. *Compos Part A Appl Sci Manuf*. 2016;83:89-97. doi:10.1016/j.compositesa.2015.05.024

55. Bondeson D, Oksman K. Polylactic acid/cellulose whisker nanocomposites modified by polyvinyl alcohol. doi:10.1016/j.compositesa.2007.08.001

56. Peng J, Walsh PJ, Sabo RC, Turng LS, Clemons CM. Water-assisted compounding of cellulose nanocrystals into polyamide 6 for use as a nucleating agent for microcellular foaming. *Polymer (Guildf)*. 2016;84:158-166. doi:10.1016/j.polymer.2015.12.050

57. Karger-Kocsis J, Kmetty Á, Lendvai L, Drakopoulos SX, Bárány T. Water-Assisted Production of Thermoplastic Nanocomposites: A Review. *Materials (Basel)*. 2015;8:72-95. doi:10.3390/ma8010072

58. Yasim-Anuar TAT, Ariffin H, Norrrahim MNF, et al. Well-dispersed cellulose nanofiber in low density polyethylene nanocomposite by liquid-Assisted extrusion. *Polymers (Basel)*. 2020;12(4):927. doi:10.3390/POLYM12040927

59. Strong AB. *Plastics: Materials and Processing*. 3rd ed. Pearson Prentice Hall; 2006.

60. Bryce D. *Plastic Injection Molding: Manufacturing Process Fundamentals*. Vol 1. Society of Manufacturing Engineers; 1996.

61. Materials – European Bioplastics. Accessed October 6, 2020. https://www.european-bioplastics.org/bioplastics/materials/

62. Hasani M, Cranston ED, Westman G, Gray DG. Cationic surface functionalization of cellulose nanocrystals. *Soft Matter*. 2008;4(11):2238-2244. doi:10.1039/b806789a

63. Chattopadhyay S, Keul H, Moeller M. Functional Polymers Bearing Reactive Azetidinium Groups: Synthesis and Characterization. *Macromol Chem Phys*. 2012;213(5):500-512.

doi:10.1002/macp.201100480

64. Dong XM, Revol JF, Gray DG. Effect of microcrystallite preparation conditions on the formation of colloid crystals of cellulose. *Cellulose*. 1998;5(1):19-32. doi:10.1023/A:1009260511939

65. Krishna Reddy VVRM, Udaykiran D, Chintamani US, Mahesh Reddy E, Kameswararao C, Madhusudhan G. Development of an optimized process for the preparation of 1-benzylazetidin-3-ol: An industrially important intermediate for substituted azetidine. *Org Process Res Dev*. 2011;15(2):462-466. doi:10.1021/op100247m

66. Parzuchowski PG, Świderska A, Roguszewska M, Frączkowski T, Tryznowski M. Amine functionalized polyglycerols obtained by copolymerization of cyclic carbonate monomers. *Polymer (Guildf)*. 2018;151:250-260. doi:10.1016/j.polymer.2018.07.055

67. Venkatesh A, Thunberg J, Moberg T, et al. Cellulose nanofibril-reinforced composites using aqueous dispersed ethylene-acrylic acid copolymer. *Cellulose*. 2018;25(8):4577-4589. doi:10.1007/s10570-018-1875-3

68. Allen NS, Lo D, Sharif Salim M, Jennings P. Influence of amine structure on the post-cured photo-yellowing of novel amine diacrylate terminated ultraviolet and electron beam cured coatings. *Polym Degrad Stab*. 1990;28(1):105-114. doi:10.1016/0141-3910(90)90055-C

69. Xiao P, Shi S, Nie J. Synthesis and characterization of copolymerizable one-component type II photoinitiator. *Polym Adv Technol*. 2008;19(9):1305-1310. doi:10.1002/pat.1132

70. Tadmor Z, Gogos CG. *Principles of Polymer Processing*. Second. John Wiley & Sons; 2006.

71. Sahlin K, Forsgren L, Moberg T, Bernin D, Rigdahl M, Westman G. Surface treatment of cellulose nanocrystals (CNC): effects on dispersion rheology. *Cellulose*. 2018;25(1):331-345. doi:10.1007/s10570-017-1582-5

72. Pisciotti F, Boldizar A, Rigdahl M, Ariño I. Effects of injection-molding conditions on the gloss and color of pigmented polypropylene. *Polym Eng Sci*. 2005;45(12):1557-1567. doi:10.1002/pen.20358

73. Gregorová A, Cibulková Z, Košíková B, Šimon P. Stabilization effect of lignin in polypropylene and recycled polypropylene. *Polym Degrad Stab*. 2005;89(3):553-558. doi:10.1016/j.polymdegradstab.2005.02.007

74. Kirschweng B, Tátraaljai D, Földes E, Pukánszky B. Natural antioxidants as stabilizers for polymers. *Polym Degrad Stab*. 2017;145:25-40. doi:10.1016/j.polymdegradstab.2017.07.012

75. Peng Y, Liu R, Cao J. Characterization of surface chemistry and crystallization behavior of polypropylene composites reinforced with wood flour, cellulose, and lignin during accelerated weathering. *Appl Surf Sci*. 2015;332:253-259. doi:10.1016/j.apsusc.2015.01.147

76. Albertsson AC, Barenstedt C, Karlsson S. Susceptibility of enhanced environmentally degradable polyethylene to thermal and photo-oxidation. *Polym Degrad Stab*. 1992;37(2):163-171. doi:10.1016/0141-3910(92)90080-O

77. Corrales T, Catalina F, Peinado C, Allen NS, Fontan E. Photooxidative and thermal degradation of polyethylenes: Interrelationship by chemiluminescence, thermal gravimetric analysis and FTIR data. *J Photochem Photobiol A Chem*. 2002;147(3):213-224.

doi:10.1016/S1010-6030(01)00629-3

78. Gulmine J V., Janissek PR, Heise HM, Akcelrud L. Degradation profile of polyethylene after artificial accelerated weathering. *Polym Degrad Stab*. 2003;79(3):385-397. doi:10.1016/S0141-3910(02)00338-5

79. Khabbaz F, Albertsson AC, Karlsson S. Chemical and morphological changes of environmentally degradable polyethylene films exposed to thermo-oxidation. *Polym Degrad Stab*. 1999;63(1):127-138. doi:10.1016/S0141-3910(98)00082-2

80. Chen Y, Xu C, Huang J, Wu D, Lv Q. Rheological properties of nanocrystalline cellulose suspensions. *Carbohydr Polym*. 2017;157:303-310. doi:10.1016/j.carbpol.2016.10.002

81. Townsend AK, Wilson HJ. Small- and large-amplitude oscillatory rheometry with bead–spring dumbbells in Stokesian Dynamics to mimic viscoelasticity. *J Nonnewton Fluid Mech*. 2018;261:136-152. doi:10.1016/j.jnnfm.2018.08.010

82. Khoshkava V, Kamal MR. Effect of cellulose nanocrystals (CNC) particle morphology on dispersion and rheological and mechanical properties of polypropylene/CNC nanocomposites. *ACS Appl Mater Interfaces*. 2014;6(11):8146-8157. doi:10.1021/am500577e

83. Sharif-Pakdaman A, Morshedian J, Jahani Y. Influence of the silane grafting of polyethylene on the morphology, barrier, thermal, and rheological properties of high-density polyethylene/organoclay nanocomposites. *J Appl Polym Sci*. 2012;125(S1):E305-E313. doi:10.1002/app.36367

84. Nielsen L. *Mechanical Properties of Polymers and Composites* . Vol 2. Marcel Dekker Inc; 1974. doi:10.1002/pol.1975.130130214

85. Matthews FL, Rawlings R. *Composite Materials: Engineering and Science*. Woodhead Publishing Limited; 1994.

86. McCrum NG, Buckley CP, Bucknall CB. *Principles of Polymer Engineering* . 2nd ed. Oxford University Press; 1997.

87. Tanpichai S, Quero F, Nogi M, et al. Effective young's modulus of bacterial and microfibrillated cellulose fibrils in fibrous networks. *Biomacromolecules*. 2012;13(5):1340-1349. doi:10.1021/bm300042t

88. Ansari F, Galland S, Johansson M, Plummer CJG, Berglund LA. Cellulose nanofiber network for moisture stable, strong and ductile biocomposites and increased epoxy curing rate. *Compos Part A Appl Sci Manuf*. 2014;63:35-44. doi:10.1016/j.compositesa.2014.03.017

89. Ansari F, Skrifvars M, Berglund L. Nanostructured biocomposites based on unsaturated polyester resin and a cellulose nanofiber network. *Compos Sci Technol*. 2015;117:298-306. doi:10.1016/j.compscitech.2015.07.004

90. Kubát J, Rigdahl M, Welander M. Characterization of interfacial interactions in high density polyethylene filled with glass spheres using dynamic-mechanical analysis. *J Appl Polym Sci*. 1990;39(7):1527-1539. doi:10.1002/app.1990.070390711

91. Yang Y, Boom R, Irion B, van Heerden DJ, Kuiper P, de Wit H. Recycling of composite materials. *Chem Eng Process Process Intensif*. 2012;51:53-68. doi:10.1016/j.cep.2011.09.007